Spectral functions of two-band spinless fermion and single-band spin-$\frac{1}{2}$ fermion models

E. Orignac
Laboratoire de Physique de l'ENS-Lyon, CNRS UMR 5672, 46 Allée d'Italie, F-69364 Lyon Cedex 07, France

M. Tsuchiizu and Y. Suzumura
Department of Physics, Nagoya University, Nagoya 464-8602, Japan
(Received 15 July 2011; revised manuscript received 23 September 2011; published 25 October 2011)

We examine zero-temperature one-particle spectral functions for the one-dimensional two-band spinless fermions with different velocities and general forward-scattering interactions. By using the bosonization technique and diagonalizing the model to two Tomonaga-Luttinger liquid Hamiltonians, we obtain general expressions for the spectral functions, which are given in terms of the Appell hypergeometric functions. For the case of identical two-band fermions, corresponding to the SU(2) symmetric spin-1/2 fermions with repulsive interactions, the spectral functions can be expressed in terms of the Gauss hypergeometric function and are shown to recover the double-peak structure suggesting the well-known "spin-charge" separation. By tuning the difference in velocities for the two-band fermions, we clarify the crossover in spectral functions from the spin-charge separation to the decoupled fermions. We discuss the relevance of our results to the spin-1/2 Hubbard model under a magnetic field, which can be mapped onto two-band spinless fermions.

DOI: 10.1103/PhysRevB.84.165128 PACS number(s): 71.10.Pm, 71.10.Fd, 79.60.−i, 67.85.Lm

I. INTRODUCTION

The physical properties of interacting fermions in three dimensions can be described using the Landau Fermi liquid concept of fermionic quasiparticles with renormalized masses and weak effective interactions.[1,2] In one dimension, the Landau Fermi liquid concept is not applicable, and interacting spin-1/2 fermions are described within the Tomonaga-Luttinger (TL) liquid concept, in which quasiparticles are replaced by collective density (or charge for electrons) and spin excitations propagating independently with respective velocities u_ρ and u_σ, the so-called spin-charge separation phenomenon.[3–7] Moreover, in the TL liquid, the single-fermion excitations are unstable and decay into collective modes, leading to the sharp suppression in the density of states.[8] Originally, candidate systems for the observation of TL liquid physics have been quasi-one-dimensional conductors, such as the first molecular conductor TTF-TCNQ,[9,10] the Fabre and Bechgaard salts,[11] the blue and purple bronzes, and carbon nanotubes.[12] Angle-resolved photoemission spectroscopy (ARPES) experiments in quasi-one-dimensional conductors have been used to measure electron spectral functions and probe their TL liquid features.[9,13–22] Self-assembled one-dimensional metallic chains of atoms on semiconductor surfaces have also been considered as potential candidates for the observation of TL liquid and spin-charge separation.[23,24] Initially, the ARPES measurement for gold atom chains on silicon surfaces revealed a double-band structure and the spin-charge separation was suggested for its origin.[25,26] However, recent spin-resolved ARPES experiments on this system[27] have shown that the double-band nature originates in the spin splitting caused by the Rashba effect. Besides ARPES, magnetotunneling measurements between a wire and a two-dimensional electron gas[28,29] or between two wires[30] are also sensitive to the TL liquid features of the spectral functions. Experiments on quantum wires[31,32] have partially confirmed the presence of TL liquid effects in tunneling current measurements. More recently, it has been proposed that ultracold atomic gases were also candidates for the observation of the TL liquid and spin-charge separation.[33–35] Indeed, atom trapping technology, either optical[36–38] or magnetic,[39,40] has permitted the realization of one-dimensional systems of interacting particles. In parallel, mixtures of bosonic and fermionic atoms,[41,42] heteronuclear mixtures of fermionic atoms,[43,44] as well as pseudospin-1/2 fermionic atoms[45] have been trapped and cooled. Recently, partially polarized pseudospin-1/2 fermionic atoms have been trapped in an array of 1D tubes.[46] Finally, an analog of photoemission spectroscopy for cold atomic gases has been developed.[47,48] These developments might permit the future measurement of spectral functions of one-dimensional trapped atomic gases and a comparison with theoretical predictions. From the theoretical point of view, spectral functions $A(q,\omega)$ for the TL liquid at $T=0$ have been considered in Refs. 49 and 50. Power-law singularities with exponents depending on the TL-liquid parameters have been predicted at $\omega = \pm u_\nu |q|$ ($\nu = \rho,\sigma$). At $T>0$, the spectral function, $A(q,\omega)$, is strongly affected by the thermal fluctuation, which reduces the effect of interaction. Actually, double peaks due to the spin-charge separation move to a single peak with increasing temperature.[51] The spectral function of the Hubbard model in one dimension has been investigated in the limit of $U \to +\infty$[52,53] with the help of the Ogata-Shiba wave function.[54] More recently, combining a bosonization approach for the charge degree of freedom and an exact treatment of the spin degrees of freedom has permitted one to obtain an analytic expression of the spectral function in that limit.[55] For finite U, the Hubbard model has been considered using exact diagonalizations,[56] quantum Monte Carlo,[57,58] and dynamical density-matrix renormalization-group methods.[59,60] The spectral functions of a magnetized TL liquid have been studied analytically[61,62] as well as numerically.[63] In the present paper, we calculate the fermion spectral function in a two-component TL liquid for zero temperature. In Sec. II, we recall the bosonization treatment of the two-band spinless fermion model,[64] and derive the expression of the real-space fermion Green's function at zero temperature. The bosonized Hamiltonian of the two-band spinless fermion models also describes spin-1/2 fermions in a magnetic field[65–67] and mixtures of spinless fermions with bosons or fermions.[68,69] In Sec. IV, the spectral functions are obtained. In the case of an SU(2) invariant model, corresponding to a TL liquid of spin-1/2 fermions in the absence of magnetic field, the fermion spectral function can be expressed in terms of the Gauss hypergeometric function as shown in Ref. 70. In the non-SU(2) invariant case, which might be achieved experimentally with polarized spin-1/2 neutral fermions,[46] or quantum wires under a magnetic field,[31] the fermion spectral functions can be expressed in terms of Appell hypergeometric functions. Our approach recovers the previous results,[49,50] but also allows us to describe the behavior of the spectral function away from the points $\omega = \pm u_\nu q$. We discuss the applications of our results to the Hubbard model under a magnetic field in Sec. IV B 3.

II. BOSONIZATION

We consider a general two-band model of interacting spinless fermions defined by

$$H = -i \sum_{a=1,2} \int dx\, v_a(\psi^\dagger_{R,a}\partial_x\psi_{R,a} - \psi^\dagger_{L,a}\partial_x\psi_{L,a}) + \sum_a \int dx\, g_a\rho_a^2 + g\int dx\, \rho_1\rho_2, \tag{2.1}$$

where $\psi_{R,a}$ and $\psi_{L,a}$ respectively annihilate one right-moving and left-moving fermion in band a, $\rho_a = \psi^\dagger_{R,a}\psi_{R,a} + \psi^\dagger_{L,a}\psi_{L,a}$, v_a is the velocity of fermions in band $a \in \{1,2\}$, and g_a is the strength of interband interaction. The model includes only the forward-scattering interaction and not the backward scattering $\sim\psi^\dagger_{R,1}\psi_{L,1}\psi^\dagger_{L,2}\psi_{R,2}$. This assumption is justified when the two bands have different Fermi wave vectors or when the backward-scattering interactions are irrelevant. The model (2.1) can be bosonized perturbatively, yielding

$$H = \sum_{a=1,2}\int \frac{dx}{2\pi}\left[u_a K_a(\pi\Pi_a)^2 + \frac{u_a}{K_a}(\partial_x\phi_a)^2\right] + \frac{g}{\pi^2}\int dx\, \partial_x\phi_1\partial_x\phi_2, \tag{2.2}$$

with $[\phi_a(x),\Pi_b(x')] = i\delta_{a,b}\delta(x-x')$ and $a,b \in \{1,2\}$. In Eq. (2.2), we have

$$u_a^2 = v_a\left(v_a + \frac{2g_a}{\pi}\right), \tag{2.3a}$$

$$K_a = \left(1 + \frac{2g_a}{\pi v_a}\right)^{-1/2}. \tag{2.3b}$$

The intraband interaction is included in K_1 and K_2. The case $K_a < 1$ ($K_a > 1$) corresponds to the repulsive (attractive) interaction. More general models (for instance, lattice models) can also be considered with bosonization. A nonperturbative formulation leads to a Hamiltonian[71]

$$H = \sum_{a,b}\int \frac{dx}{2\pi}[\pi^2 M_{ab}\Pi_a\Pi_b + N_{ab}\partial_x\phi_a\partial_x\phi_b], \tag{2.4}$$

where the matrices M and N are real symmetric and are defined in terms of the variations of the ground-state energy $E_{\rm GS}$ of a finite system of size L from (respectively) change of boundary conditions $\psi_a(L) = e^{i\varphi_a}\psi_a(0)$ and change of particle densities $\rho_a = N_a/L$:

$$M_{ab} = \pi L\frac{\partial^2 E_{\rm GS}}{\partial\varphi_a\partial\varphi_b}, \tag{2.5}$$

$$N_{ab} = \frac{1}{\pi L}\frac{\partial^2 E_{\rm GS}}{\partial\rho_a\partial\rho_b}. \tag{2.6}$$

The spectrum of the general bosonized Hamiltonian (2.4) is obtained by a linear transformation of the fields Π_a and ϕ_a:

$$\Pi_b = \sum_\beta P_{b\beta}\tilde\Pi_\beta, \tag{2.7}$$

$$\phi_a = \sum_\alpha Q_{a\alpha}\tilde\phi_\alpha, \tag{2.8}$$

where $P\,{}^tQ = 1$ in order to preserve the canonical commutation relations.[72] The matrices P and Q are calculated explicitly by applying a succession of linear transformations. First, the matrix M is diagonalized by a rotation R_1 ($\Delta_1 = {}^tR_1MR_1$) which transforms the matrix N into $N_1 = {}^tR_1NR_1$. Hereafter, we denote $\boldsymbol\phi = {}^t(\phi_1,\phi_2)$ and $\boldsymbol\Pi = {}^t(\Pi_1,\Pi_2)$. By the transformation $\boldsymbol\Pi = R_1\boldsymbol\Pi_1$ and $\boldsymbol\phi = R_1\boldsymbol\phi_1$, the Hamiltonian is thus transformed into

$$H = \int\frac{dx}{2\pi}[\pi^{2\,t}\boldsymbol\Pi_1\Delta_1\boldsymbol\Pi_1 + {}^t(\partial_x\boldsymbol\phi_1)N_1(\partial_x\boldsymbol\phi_1)]. \tag{2.9}$$

Using a second transformation $\boldsymbol\Pi_1 = \Delta_1^{-1/2}\boldsymbol\Pi_2$ and $\boldsymbol\phi_1 = \Delta_1^{1/2}\boldsymbol\phi_2$, the Hamiltonian becomes

$$H = \int\frac{dx}{2\pi}\left[\pi^{2\,t}\boldsymbol\Pi_2\boldsymbol\Pi_2 + {}^t(\partial_x\boldsymbol\phi_2)\Delta_1^{1/2}N_1\Delta_1^{1/2}(\partial_x\boldsymbol\phi_2)\right]. \tag{2.10}$$

As the matrix $\Delta_1^{1/2}N_1\Delta_1^{1/2}$ is symmetric, it can be diagonalized by a rotation R_2, i.e., $\Delta_1^{1/2}N_1\Delta_1^{1/2} = R_2\Delta_2{}^tR_2$. Writing $\boldsymbol\Pi_2 = R_2\boldsymbol\Pi_3$ and $\boldsymbol\phi_2 = R_2\boldsymbol\phi_3$, we find that the Hamiltonian can be diagonalized as

$$H = \int\frac{dx}{2\pi}[\pi^{2\,t}\boldsymbol\Pi_3\boldsymbol\Pi_3 + {}^t(\partial_x\boldsymbol\phi_3)\Delta_2(\partial_x\boldsymbol\phi_3)], \tag{2.11}$$

in which the modes are decoupled. Finally, we can rescale the fields $\boldsymbol\Pi_3 = (\Delta_2)^{1/4}\tilde{\boldsymbol\Pi}$ and $\boldsymbol\phi_3 = (\Delta_2)^{-1/4}\tilde{\boldsymbol\phi}$ to write

$$H = \int\frac{dx}{2\pi}[\pi^{2\,t}\tilde{\boldsymbol\Pi}(\Delta_2)^{1/2}\tilde{\boldsymbol\Pi} + {}^t(\partial_x\tilde{\boldsymbol\phi})(\Delta_2)^{1/2}(\partial_x\tilde{\boldsymbol\phi})]. \tag{2.12}$$

In this last equation, the elements on the diagonal of $(\Delta_2)^{1/2}$ are the velocities u_β of the decoupled modes of the Hamiltonian (2.4). The stability of the multicomponent TL liquid state requires that the velocities in Eq. (2.11) are real, i.e., that the matrix MN has only positive eigenvalues. The transformations can be written explicitly as

$$P = R_1\Delta_1^{-1/2}R_2(\Delta_2)^{1/4}, \tag{2.13}$$

$$Q = R_1\Delta_1^{1/2}R_2(\Delta_2)^{-1/4}, \tag{2.14}$$

and we have ${}^tPMP = (\Delta_2)^{1/2}$ and ${}^tQNQ = (\Delta_2)^{1/2}$. This implies in particular that: ${}^tPMNQ = \Delta_2$, i.e., $Q^{-1}MNQ = \Delta_2$ and, by taking the transpose, $P^{-1}NMP = \Delta_2$. The excitation velocities $u_\pm$ where $\Delta_2 = \mathrm{diag}(u_+^2,u_-^2)$ are obtained as

$$u_{\pm}^2 = \frac{u_1^2+u_2^2}{2} + M_{12}N_{12} \pm \sqrt{\left(\frac{u_1^2-u_2^2}{2}\right)^2 + (M_{11}N_{12}+M_{12}N_{22})(M_{21}N_{11}+M_{22}N_{21})}, \quad (2.15)$$

where $u_1^2 \equiv N_{11}M_{11}$ and $u_2^2 \equiv N_{22}M_{22}$. The diagonalization method allows us to derive also expressions for the Green's functions of the chiral fields,

$$\begin{aligned} \phi_{R,a} &= \phi_a - \theta_a, & \tilde{\phi}_{R,a} &= \tilde{\phi}_a - \tilde{\theta}_a, \\ \phi_{L,a} &= \phi_a + \theta_a, & \tilde{\phi}_{L,a} &= \tilde{\phi}_a + \tilde{\theta}_a, \end{aligned} \quad (2.16)$$

where $\theta_a = \pi \int^x dx' \Pi_a(x')$. The field operators are expressed as

$$\psi_{R,a}(x,t) = \frac{1}{\sqrt{2\pi\alpha}} e^{-i\phi_{R,a}(x,t)}, \quad (2.17a)$$

$$\psi_{L,a}(x,t) = \frac{1}{\sqrt{2\pi\alpha}} e^{i\phi_{L,a}(x,t)}, \quad (2.17b)$$

where α is the short-distance cutoff. The Hamiltonian (2.12) can be reexpressed in terms of noninteracting chiral fields,

$$H = \int \frac{dx}{4\pi} \left[{}^t(\partial_x \tilde{\boldsymbol{\phi}}_R) \Delta_2^{1/2} (\partial_x \tilde{\boldsymbol{\phi}}_R) + {}^t(\partial_x \tilde{\boldsymbol{\phi}}_L) \Delta_2^{1/2} (\partial_x \tilde{\boldsymbol{\phi}}_L) \right], \quad (2.18)$$

with the transformation

$$\boldsymbol{\phi}_R = \tfrac{1}{2}[(Q+P)\tilde{\boldsymbol{\phi}}_R + (Q-P)\tilde{\boldsymbol{\phi}}_L], \quad (2.19)$$

$$\boldsymbol{\phi}_L = \tfrac{1}{2}[(Q-P)\tilde{\boldsymbol{\phi}}_R + (Q+P)\tilde{\boldsymbol{\phi}}_L], \quad (2.20)$$

where $\tilde{\boldsymbol{\phi}}_R = {}^t(\phi_{R,1},\phi_{R,2})$ and $\tilde{\boldsymbol{\phi}}_L = {}^t(\phi_{L,1},\phi_{L,2})$.

For the model (2.1), the off-diagonal term of N is given by $N_{12} = g/\pi$ and there is no interband current-current interaction, i.e., $M_{12} = 0$. In this case, the explicit forms of the matrices P and Q for the model (2.1) can be expressed in a compact form. Since $M_{12} = 0$, the matrix R_1 becomes unit matrix, and $\Delta_1 = M = \mathrm{diag}(u_1K_1, u_2K_2)$. The matrix Δ_2 is given by $\Delta_2 = \mathrm{diag}(u_+^2, u_-^2)$, where

$$u_{\pm}^2 = \frac{u_1^2+u_2^2}{2} \pm \sqrt{\left(\frac{u_1^2-u_2^2}{2}\right)^2 + \left(\frac{g}{\pi}\right)^2 u_1K_1u_2K_2}. \quad (2.21)$$

We note that the velocities $u_{\pm}$ depend on g^2, i.e., do not depend on the sign of g. From Eq. (2.13), we obtain

$$P = \begin{pmatrix} \sqrt{\frac{u_+}{u_1K_1}} \cos\frac{\alpha}{2} & -\sqrt{\frac{u_-}{u_1K_1}} \sin\frac{\alpha}{2} \\ \sqrt{\frac{u_+}{u_2K_2}} \sin\frac{\alpha}{2} & \sqrt{\frac{u_-}{u_2K_2}} \cos\frac{\alpha}{2} \end{pmatrix}, \quad (2.22)$$

$$Q = \begin{pmatrix} \sqrt{\frac{u_1K_1}{u_+}} \cos\frac{\alpha}{2} & -\sqrt{\frac{u_1K_1}{u_-}} \sin\frac{\alpha}{2} \\ \sqrt{\frac{u_2K_2}{u_+}} \sin\frac{\alpha}{2} & \sqrt{\frac{u_2K_2}{u_-}} \cos\frac{\alpha}{2} \end{pmatrix}, \quad (2.23)$$

where $\tan\alpha = 2(g/\pi)\sqrt{u_1K_1u_2K_2}/(u_1^2-u_2^2)$. From Eq. (2.21), the stability condition is given by

$$u_1u_2 > \left(\frac{g}{\pi}\right)^2 K_1K_2. \quad (2.24)$$

In the following analysis, we restrict ourselves to the case of $u_1 > u_2$, and Eq. (2.24) gives the lower condition for u_2, i.e., $u_2 > u_{2c} \equiv (g/\pi)^2 K_1K_2/u_1$.

III. PHASE DIAGRAM

We derive a phase diagram for the model (2.1) by examining asymptotic behavior of correlation functions:

$$\langle O_A(x)O_A(0)\rangle \sim x^{-\eta_A}, \quad (3.1)$$

where the O_A's represent the order parameters and the η_A's the corresponding exponents. We restrict ourselves to the simplest case $g_1 = g_2$ in Eq. (2.1), and assume $v_2/v_1 \leqslant 1$ without loss of generality. In the TL-liquid state, the state with the smallest exponent represents the (quasi-) long-range-ordered state and thus we can determine the phase diagram. As possible order parameters, we can consider the intraband density wave (DW) and pairing of superconducting state (SC), which are given by $O_{\mathrm{DW}a} \propto \exp(i2\phi_a)$ and $O_{\mathrm{SC}a} \propto \exp(i2\theta_a)$. Their respective exponents η_A are given by

$$\eta_{\mathrm{DW1}} = \frac{u_1K_1}{u_+u_-}\left(u_+ + u_- - \frac{u_1^2-u_2^2}{u_+ + u_-}\right), \quad (3.2a)$$

$$\eta_{\mathrm{DW2}} = \frac{u_2K_2}{u_+u_-}\left(u_+ + u_- + \frac{u_1^2-u_2^2}{u_+ + u_-}\right), \quad (3.2b)$$

$$\eta_{\mathrm{SC1}} = \frac{1}{u_1K_1}\left(u_+ + u_- + \frac{u_1^2-u_2^2}{u_+ + u_-}\right), \quad (3.2c)$$

$$\eta_{\mathrm{SC2}} = \frac{1}{u_2K_2}\left(u_+ + u_- - \frac{u_1^2-u_2^2}{u_+ + u_-}\right). \quad (3.2d)$$

In addition, we can also consider the order parameters for the interband DW and interband SC states, given by $O_{\text{interband DW}} = \psi_{R,1}^\dagger \psi_{L,2} \propto e^{i\phi_{R,1}+i\phi_{L,2}}$ and $O_{\text{interband SC}} = \psi_{R,1}\psi_{L,2} \propto e^{-i\phi_{R,1}+i\phi_{L,2}}$. The corresponding exponents are given by

$$\begin{aligned} \eta_{\text{interband DW}} &= \frac{\eta_{\mathrm{DW1}}}{4} + \frac{\eta_{\mathrm{DW2}}}{4} + \frac{\eta_{\mathrm{SC1}}}{4} + \frac{\eta_{\mathrm{SC2}}}{4} \\ &\quad - \frac{(g/\pi)}{u_+ + u_-}\left(1 + \frac{u_1K_1u_2K_2}{u_+u_-}\right), \end{aligned} \quad (3.3a)$$

$$\begin{aligned} \eta_{\text{interband SC}} &= \frac{\eta_{\mathrm{DW1}}}{4} + \frac{\eta_{\mathrm{DW2}}}{4} + \frac{\eta_{\mathrm{SC1}}}{4} + \frac{\eta_{\mathrm{SC2}}}{4} \\ &\quad + \frac{(g/\pi)}{u_+ + u_-}\left(1 + \frac{u_1K_1u_2K_2}{u_+u_-}\right). \end{aligned} \quad (3.3b)$$

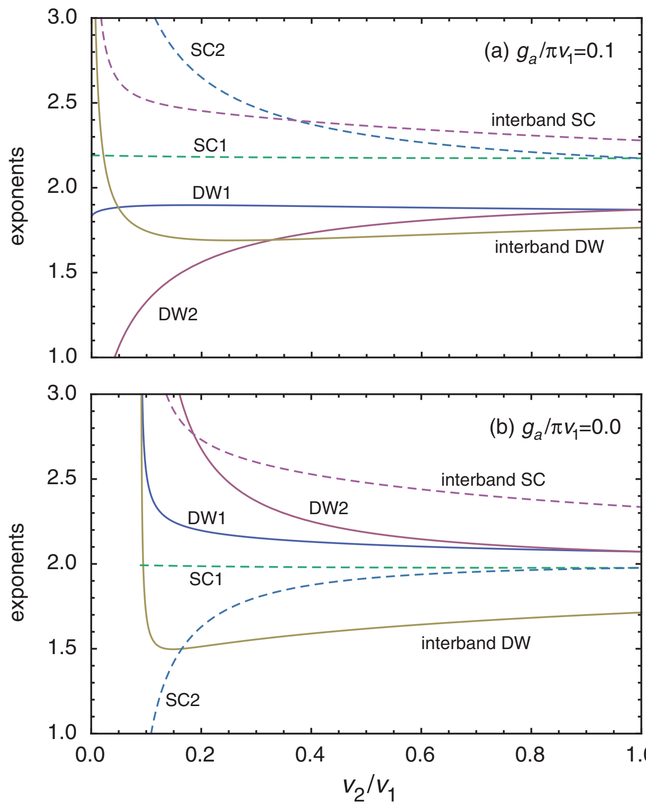

FIG. 1. (Color online) Exponents η_A for possible order parameters as a function of v_2/v_1 for $g_a/(\pi v_1) = 0.1$ (a) and $g_a/(\pi v_1) = 0.0$ (b) with fixed $g/(\pi v_1) = 0.3$.

In Fig. 1, these exponents are shown as a function of v_2/v_1, for repulsive interactions. For $v_2/v_1 = 1$, the interband DW state becomes dominant if $g > 2g_a$ [see Fig. 1(a)], while the DW2 state becomes dominant if $g < 2g_a$. For decreasing v_2, the interband DW state is unfavorable and instead the DW2 state becomes dominant, since the effect of the intraband interaction g_a/v_2 is enhanced. On the other hand, if the intraband interactions are absent ($g_a = 0$) [see Fig. 1(b)], the DW2 state is no longer enhanced for small v_2 and instead the exponent η_{SC2} decreases with decreasing v_2 and the SC2 state becomes the most dominant state and finally the two-component TLL state becomes unstable ($u_-^2 < 0$). In Fig. 2, the phase diagram on the plane of v_2/v_1 and $g_a/(\pi v_1)$ is shown with fixed $g/(\pi v_1) = 0.3$. In the analogy to the spinful electron model, the DW2, interband DW, and SC2 states correspond to the conventional charge-density-wave, spin-density-wave, and triplet SC states, respectively. The region of the interband DW state becomes narrow with decreasing v_2 and shrinks at the point $[v_2/v_1, g_a/(\pi v_1)] \approx (0,0.04)$, where the SC2, DW2, and interband DW states have the same exponent. We note that, for $g = 0$, we can recover the behavior that the DW2 state becomes dominant for $g_a > 0$, while the SC2 state becomes dominant for $-\pi v_2/2 < g_a < 0$, and the system becomes unstable if $g_a < -\pi v_2/2$. We note that the expressions (2.3) are valid only for weak interactions, and thus the precise determination of phase diagram for the region $g_a/v_2 \gg 1$ in Fig. 2 is beyond

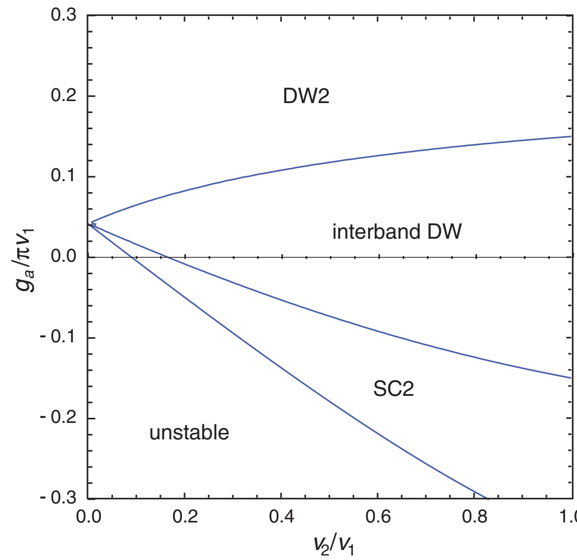

FIG. 2. (Color online) Phase diagram on a plane of v_2/v_1 and $g_a/(\pi v_1)$ with fixed $g/(\pi v_1) = 0.3$. In the "unstable" region, u_2 becomes imaginary.

the present approach. From the qualitative considerations, the following modifications to the phase diagram can be expected. Since the parameter K_2 would take a nonzero value for $g_a/v_2 \to \infty$, the condition (2.24) cannot be fulfilled for small v_2/v_1, and then the unstable region always appears in the small limit of v_2/v_1 for all values of g_a. Furthermore, by noting that the unstable region is adjacent to the SC2 state, it is expected that the SC2 state is obtained even for large g_a region and is located in between the DW2 state and the unstable region.

IV. SPECTRAL FUNCTION

The spectral function is obtained from

$$A_a(k,\omega) = -\frac{1}{\pi}\mathrm{Im}\int dx\,dt\,e^{-i(kx-\omega t)}G_a(x,t), \tag{4.1}$$

where $G_a(x,t)$ is the retarded fermion Green's function $G_a(x,t) = -i\theta(t)\langle\{\psi_a(x,t),\psi_a^\dagger(0,0)\}\rangle$. Introducing the right-moving and left-moving components, $\psi_a(x,t) = e^{ik_{F,a}x}\psi_{R,a}(x,t) + e^{-ik_{F,a}x}\psi_{L,a}(x,t)$, the chiral Green's functions ($\nu = R,L$) are given by

$$G_{\nu,a}(x,t) = -i\theta(t)[F_{\nu,a}(x,t) + F_{\nu,a}(-x,-t)], \tag{4.2}$$

where $F_{\nu,a}(x,t) = \langle\psi_{\nu,a}(x,t)\psi_{\nu,a}^\dagger(0,0)\rangle$. Then the spectral function can be decomposed into the four contributions:

$$\begin{aligned} A_a(k,\omega) &= A_{R,a}(k - k_{F,a},\omega) + A_{L,a}(k + k_{F,a},\omega), \\ A_{\nu,a}(q,\omega) &= I_{\nu,a}(q,\omega) + I_{\nu,a}(-q,-\omega), \end{aligned} \tag{4.3}$$

where

$$I_{\nu,a}(q,\omega) = \frac{1}{2\pi}\int_{-\infty}^{\infty} dt\, e^{i\omega t}\int_{-\infty}^{\infty} dx\, e^{-iqx} F_{\nu,a}(x,t). \tag{4.4}$$

The direct calculation of the Green's functions for the phase variables yields

$$\begin{aligned}\langle[\theta_a(x,t) - \phi_a(x,t)][\theta_a(0,0) - \phi_a(0,0)]\rangle_{\rm conn} \\ = \sum_{\beta=\pm} \nu_{a,\beta} \ln\left[\frac{\alpha}{\alpha + i(u_\beta t - x)}\right] \\ + \nu'_{a,\beta} \ln\left[\frac{\alpha}{\alpha + i(u_\beta t + x)}\right],\end{aligned} \tag{4.5}$$

$$\begin{aligned}\langle[\theta_a(x,t) + \phi_a(x,t)][\theta_a(0,0) + \phi_a(0,0)]\rangle_{\rm conn} \\ = \sum_{\beta=\pm} \nu'_{a,\beta} \ln\left[\frac{\alpha}{\alpha + i(u_\beta t - x)}\right] \\ + \nu_{a,\beta} \ln\left[\frac{\alpha}{\alpha + i(u_\beta t + x)}\right],\end{aligned} \tag{4.6}$$

where the exponents ν are given by

$$\nu_{a,\beta} = \tfrac{1}{4}(P_{a\beta} + Q_{a\beta})^2, \quad \nu'_{a,\beta} = \tfrac{1}{4}(P_{a\beta} - Q_{a\beta})^2. \tag{4.7}$$

Thus the one-particle Green's functions are expressed as

$$\begin{aligned}\langle\psi_{R,a}(x,t)\psi^\dagger_{R,a}(0,0)\rangle = \frac{1}{2\pi\alpha}\prod_\beta\left[\frac{\alpha}{\alpha + i(u_\beta t - x)}\right]^{\nu_{a,\beta}} \\ \times\left[\frac{\alpha}{\alpha + i(u_\beta t + x)}\right]^{\nu'_{a,\beta}},\end{aligned} \tag{4.8a}$$

$$\begin{aligned}\langle\psi_{L,a}(x,t)\psi^\dagger_{L,a}(0,0)\rangle = \frac{1}{2\pi\alpha}\prod_\beta\left[\frac{\alpha}{\alpha + i(u_\beta t - x)}\right]^{\nu'_{a,\beta}} \\ \times\left[\frac{\alpha}{\alpha + i(u_\beta t + x)}\right]^{\nu_{a,\beta}}.\end{aligned} \tag{4.8b}$$

Substituting the expression from Eq. (4.8) into Eq. (4.4), we obtain the integral form for the spectral function. We note that we have the identity $\sum_\beta(\nu_{a,\beta} - \nu'_{a,\beta}) = 1$. The spectral function is obtained from the integral

$$I_{R,a}(q,\omega) = \frac{\alpha^{\bar\nu_a - 1}}{(2\pi)^2}\int dx\, dt \frac{e^{i(\omega t - qx)}}{[\alpha + i(u_+t - x)]^{\nu_{a,+}}[\alpha + i(u_-t - x)]^{\nu_{a,-}}[\alpha + i(u_+t + x)]^{\nu'_{a,+}}[\alpha + i(u_-t + x)]^{\nu'_{a,-}}}, \tag{4.9}$$

where $\bar\nu_a \equiv (\nu_{a,+} + \nu_{a,-} + \nu'_{a,+} + \nu'_{a,-})$. A similar expression for left-moving fermions has $\nu_{a,\pm}$ and $\nu'_{a,\pm}$ interchanged.

A. SU(2) symmetric model

Let us first consider the case with SU(2) symmetry and repulsive interactions, and show how the expressions in terms of Gauss hypergeometric functions are recovered.[70] The bosonized Hamiltonian reads $H = H_\rho + H_\sigma$, where

$$H_\rho = \int\frac{dx}{2\pi}\left[u_\rho K_\rho(\pi\Pi_\rho)^2 + \frac{u_\rho}{K_\rho}(\partial_x\phi_\rho)^2\right], \tag{4.10}$$

$$\begin{aligned}H_\sigma = \int\frac{dx}{2\pi}\left[u_\sigma K_\sigma(\pi\Pi_\sigma)^2 + \frac{u_\sigma}{K_\sigma}(\partial_x\phi_\sigma)^2\right] \\ + \frac{2g_{1\perp}}{(2\pi\alpha)^2}\int dx\, \cos\sqrt{8}\phi_\sigma,\end{aligned} \tag{4.11}$$

with $u_\rho > u_\sigma$, $K_\rho < 1$, and $K_\sigma > 1$ for repulsive interactions. Under the renormalization group, $K_\sigma, g_{1\perp}$ flow to fixed-point values $K^*_\sigma = 1, g^*_{1\perp} = 0$. The resulting fixed-point Hamiltonian is therefore in the diagonalized form of Eq. (2.12). We will approximate the spectral function of this model by replacing the exact Green's function by its fixed-point value. This amounts to neglecting logarithmic corrections. Within this approximation, the spectral function of right-moving fermions of spin $s = \uparrow, \downarrow$ is given by $A_{R,s}(q,\omega) = I_R(q,\omega) + I_R(-q, -\omega)$, with

$$\begin{aligned}I_R(q,\omega) = \frac{\alpha^{2\gamma_\rho}}{(2\pi)^2}\int dx\, dt\, e^{i(\omega t - qx)} \\ \times\frac{1}{[\alpha + i(u_\rho t - x)]^{\gamma_\rho + 1/2}}\frac{1}{[\alpha + i(u_\sigma t - x)]^{1/2}} \\ \times\frac{1}{[\alpha + i(u_\rho t + x)]^{\gamma_\rho}},\end{aligned} \tag{4.12}$$

where $\gamma_\rho = (K_\rho + K_\rho^{-1} - 2)/8$. (Actually, we could consider the more general case of a SU(N) symmetric model with $N > 2$. The model still has spin-charge separation, but the spin part of the correlation decays with an exponent $(N-1)/N$ instead of $1/2$, while the charge part has exponent $(2\gamma_\rho + 1)/N$ for the right-moving factor and $2\gamma_\rho/N$ for the left-moving factor. The computation of the spectral function proceeds in exactly the same manner as in the SU(2) case, albeit with the replacement $v^{\gamma_\rho - 1/2}(1-v)^{-1/2}/\Gamma(\gamma_\rho + 1/2)\Gamma(1/2) \to v^{(2\gamma_\rho+1)/N-1}(1-v)^{-1/N}/\Gamma((2\gamma_\rho+1)/N)\Gamma(1-1/N)$ in Eq. (4.15), leading again an expression in terms of Gauss hypergeometric functions.) The correspondence between Eqs. (4.9) and (4.12) is given by $u_+ = u_\rho$, $u_- = u_\sigma$, $\nu_{a,+} = (\gamma_\rho + 1/2)$, $\nu_{a,-} = 1/2$, $\nu'_{a,+} = \gamma_\rho$, and $\nu'_{a,-} = 0$. To calculate the integral in Eq. (4.12), we use the Feynman representation:[73]

$$\frac{1}{A_1^{\nu_1}A_2^{\nu_2}}=\frac{\Gamma(\nu_1+\nu_2)}{\Gamma(\nu_1)\Gamma(\nu_2)}\int_0^1 dw\frac{w^{\nu_1-1}(1-w)^{\nu_2-1}}{[A_1w+A_2(1-w)]^{\nu_1+\nu_2}}, \tag{4.13}$$

which is valid for $\nu_1,\nu_2>0$. Then, with the help of Eq. (A4), we obtain

$$\begin{aligned}I_R(q,\omega)=&\frac{\Gamma(\gamma_\rho+1)}{4\pi^2\Gamma(\gamma_\rho+1/2)\Gamma(1/2)}\int dx\,dt\,e^{i(\omega t-qx)}\\&\times\int_0^1 dv\frac{v^{\gamma_\rho-1/2}(1-v)^{-1/2}\alpha^{\gamma_\rho}}{\{\alpha+i[vu_\rho+(1-v)u_\sigma]t-ix\}^{\gamma_\rho+1}}\\&\times\left[\frac{\alpha}{\alpha+i(u_\rho t+x)}\right]^{\gamma_\rho}.\end{aligned} \tag{4.14}$$

After the space-time integration, we have

$$\begin{aligned}I_R(q,\omega)=&\frac{\alpha^{2\gamma_\rho}}{\Gamma(\gamma_\rho+1/2)\Gamma(\gamma_\rho)\Gamma(1/2)}|\omega+u_\rho q|^{\gamma_\rho}\\&\times\int_0^1 dv\,v^{\gamma_\rho-1/2}(1-v)^{-1/2}\\&\times\frac{|\omega-[vu_\rho+(1-v)u_\sigma]q|^{\gamma_\rho-1}}{|u_\rho(1+v)+u_\sigma(1-v)|^{2\gamma_\rho}}\Theta(\omega+u_\rho q)\\&\times\Theta\{\omega-[vu_\rho+(1-v)u_\sigma]q\},\end{aligned} \tag{4.15}$$

where $\Theta(x)$ is the Heaviside step function and $\Gamma(z)$ is the Euler Γ function. We will consider the case of $q>0$. From Eq. (4.15), we find $I_R(q,\omega)=0$ for $\omega<u_\sigma q$ and $I_R(-q,-\omega)=0$ for $\omega>-u_\rho q$. Therefore, $A_{R,s}(q,\omega)=0$ when $-u_\rho q<\omega<u_\sigma q$, while $A_{R,s}(q,\omega)=I_R(q,\omega)$ for $\omega>u_\sigma q$ and $A_{R,s}(a,\omega)=I_R(-q,-\omega)$ for $\omega<-u_\rho q$. For the calculation of $I_R(q,\omega)$ when $\omega>u_\sigma q$, we have to separate the two cases: $u_\sigma q<\omega<u_\rho q$ and $\omega>u_\rho q$.

1. $\omega > u_\rho q$

For $\omega>u_\rho q$, the two Θ functions in Eq. (4.15) can be replaced by one. With the change of variable

$$w=\frac{2u_\rho v}{u_\rho+u_\sigma+(u_\rho-u_\sigma)v}, \tag{4.16}$$

the integral Eq. (4.15) becomes

$$\begin{aligned}&A_{R,s}(q,\omega)\\&=\frac{\alpha^{2\gamma_\rho}}{\Gamma(\gamma_\rho)\Gamma(\gamma_\rho+1)}\frac{(\omega+u_\rho q)^{\gamma_\rho}(\omega-u_\sigma q)^{\gamma_\rho-1}}{(2u_\rho)^{\gamma_\rho+1/2}(u_\rho+u_\sigma)^{\gamma_\rho-1/2}}\\&\quad\times{}_2F_1\left(1-\gamma_\rho,\gamma_\rho+\frac{1}{2};\gamma_\rho+1;\frac{u_\rho-u_\sigma}{2u_\rho}\frac{\omega+u_\rho q}{\omega-u_\sigma q}\right).\end{aligned} \tag{4.17}$$

For $\omega\to\infty$, $I(q,\omega)\sim\omega^{2\gamma_\rho-1}$. The expression (4.17) agrees with Eq. (19.27) of Ref. 70 with the notation $\theta=2\gamma_\rho$. When $\omega\to u_\rho q+0$, the argument of the hypergeometric function in Eq. (4.17) becomes equal to one and, for $\gamma_\rho<1/2$, the hypergeometric function is divergent. Using Eq. (A6), we rewrite Eq. (4.17) as

$$\begin{aligned}A_{R,s}(q,\omega)=&\frac{(\alpha/2u_\rho)^{2\gamma_\rho}}{\Gamma(\gamma_\rho)\Gamma(\gamma_\rho+1)}\\&\times\frac{(\omega+u_\rho q)^{\gamma_\rho}(\omega-u_\rho q)^{\gamma_\rho-1/2}}{(\omega-u_\sigma q)^{1/2}}\\&\times{}_2F_1\left(2\gamma_\rho,\frac{1}{2};\gamma_\rho+1;\frac{u_\rho-u_\sigma}{2u_\rho}\frac{\omega+u_\rho q}{\omega-u_\sigma q}\right),\end{aligned} \tag{4.18}$$

in which the hypergeometric function remains finite as $\omega\to u_\rho q+0$. We then find that $A_{R,s}(q,\omega)\sim\frac{\alpha^{2\gamma_\rho}q^{\gamma_\rho-1/2}\Gamma(1/2-\gamma_\rho)\sin(\pi\gamma_\rho)}{(2u_\rho)^{\gamma_\rho}(u_\rho-u_\sigma)^{1/2}\Gamma(1/2+\gamma_\rho)\pi}(\omega-u_\rho q)^{\gamma_\rho-1/2}$ as $\omega\sim u_\rho q$. The power-law divergence was previously obtained by Voit[50] and by Meden and Schoenhammer[49] by analyzing the divergence of the integral (4.12) in the vicinity of $\omega\sim u_\rho q$. The expression in terms of hypergeometric functions also provides the prefactors.

2. $u_\sigma q < \omega < u_\rho q$

When $u_\sigma q<\omega<u_\rho q$, the integration over v in Eq. (4.15) is limited to the range $0<v<(\omega-u_\sigma q)/(u_\rho q-u_\sigma q)$. With the change of variable,

$$w=\frac{\omega+u_\rho q}{\omega-u_\sigma q}\frac{(u_\rho-u_\sigma)v}{(u_\rho+u_\sigma)+(u_\rho-u_\sigma)v}, \tag{4.19}$$

the integral (4.15) reduces to

$$\begin{aligned}A_{R,s}(q,\omega)=&\frac{\alpha^{2\gamma_\rho}}{\Gamma(1/2)\Gamma(2\gamma_\rho+1/2)}\\&\times\frac{(\omega+u_\rho q)^{-1/2}(\omega-u_\sigma q)^{2\gamma_\rho-1/2}}{(u_\rho+u_\sigma)^{\gamma_\rho-1/2}(u_\rho-u_\sigma)^{\gamma_\rho+1/2}}\\&\times{}_2F_1\left(\frac{1}{2},\gamma_\rho+\frac{1}{2};2\gamma_\rho+\frac{1}{2};\frac{2u_\rho}{u_\rho-u_\sigma}\frac{\omega-u_\sigma q}{\omega+u_\rho q}\right).\end{aligned} \tag{4.20}$$

For $\omega\to u_\sigma q+0$, the expression (4.20) has a power-law divergence, $\sim(\omega-u_\sigma q)^{2\gamma_\rho-1/2}$ for $\gamma_\rho<1/4$, in agreement with Refs. 49 and 50. When $\omega\to u_\rho q-0$, the argument of the hypergeometric function becomes equal to one, leading to a power-law divergence. Using again Eq. (A6), we can rewrite Eq. (4.20) as

$$\begin{aligned}A_{R,s}(q,\omega)=&\frac{\alpha^{2\gamma_\rho}}{\Gamma(1/2)\Gamma(2\gamma_\rho+1/2)}\\&\times\frac{(\omega-u_\sigma q)^{2\gamma_\rho-1/2}(u_\rho q-\omega)^{\gamma_\rho-1/2}}{(\omega+u_\rho q)^{\gamma_\rho}(u_\rho-u_\sigma)^{2\gamma_\rho}}\\&\times{}_2F_1\left(2\gamma_\rho,\gamma_\rho;2\gamma_\rho+\frac{1}{2};\frac{2u_\rho}{u_\rho-u_\sigma}\frac{\omega-u_\sigma q}{\omega+u_\rho q}\right),\end{aligned} \tag{4.21}$$

and recover the divergence[49,50] $A_{R,s}\sim\frac{\alpha^{2\gamma_\rho}q^{\gamma_\rho-1/2}\Gamma(1/2-\gamma_\rho)}{(2u_\rho)^{\gamma_\rho}(u_\rho-u_\sigma)^{1/2}\Gamma(1/2+\gamma_\rho)\pi}(u_\rho q-\omega)^{\gamma_\rho-1/2}$ for $\omega\to u_\rho q-0$. Although the exponent is the same on both sides of $\omega=u_\rho q$, the peak is asymmetric, with the ratio of amplitudes being $\sin(\pi\gamma_\rho)$.

3. $\omega < -u_\rho q$

In the case $\omega < -u_\rho q$, we need $I_{R,\sigma}(-q,-\omega)$. In the integral (4.15), both Θ functions are then equal to one and, with the change of variable,

$$w = \frac{2u_\rho v}{(u_\rho + u_\sigma) + (u_\rho - u_\sigma)v}, \tag{4.22}$$

we find

$$\begin{aligned} A_{R,\sigma}(q,\omega) = {} & \frac{\alpha^{2\gamma_\rho}}{\Gamma(\gamma_\rho)\Gamma(\gamma_\rho+1)} \\ & \times \frac{|\omega - u_\sigma q|^{\gamma_\rho - 1}|\omega + u_\rho q|^{\gamma_\rho}}{(u_\rho + u_\sigma)^{\gamma_\rho - 1/2}(2u_\rho)^{\gamma_\rho + 1/2}} \\ & \times {}_2F_1\left(1-\gamma_\rho,\gamma_\rho+\frac{1}{2};\gamma_\rho+1;\frac{u_\rho - u_\sigma}{2u_\rho}\frac{\omega+u_\rho q}{\omega-u_\sigma q}\right). \end{aligned} \tag{4.23}$$

For $\omega \to -u_\rho q - 0$, the expression (4.23) vanishes with a cusp singularity $A_{R,\sigma}(-q,-\omega) \sim \frac{\alpha^{2\gamma_\rho} q^{\gamma_\rho - 1}}{(2u_\rho)^{\gamma_\rho}\Gamma(\gamma_\rho)\Gamma(\gamma_\rho+1)[2u_\rho(u_\rho+u_\sigma)]^{1/2}} |\omega + u_\rho q|^{\gamma_\rho}$, in agreement with Refs. 49 and 50.

Typical behavior of the spectral functions $A_{R,s}(q,\omega)$ is shown in Fig. 3. There is no weight at $-u_\rho q < \omega < u_\sigma q$. The overall profile reproduces the previous results given in Refs. 49 and 50. We note that, for $\gamma_\rho > 1/2$, the divergence at $\omega = u_\rho q$ disappears and is replaced by the cusp structure. From Eqs. (4.17) and (4.20), its peak value is given by

$$A_{R,s}(q,u_\rho q) = \frac{\alpha^{2\gamma_\rho}\Gamma\left(\gamma_\rho - \frac{1}{2}\right)}{\Gamma(\gamma_\rho)\Gamma(2\gamma_\rho)\Gamma\left(\frac{1}{2}\right)} \frac{(\Delta u)^{\gamma_\rho - 1} q^{2\gamma_\rho - 1}}{(2u_\rho)^{1/2}(2\bar{u})^{\gamma_\rho - 1/2}}, \tag{4.24}$$

where $\bar{u} = (u_\rho + u_\sigma)/2$ and $\Delta u = (u_\rho - u_\sigma)$. In Fig. 3, the peak positions are represented by the dots. Thus the asymptotic behavior at $\omega \approx u_\rho q$ for $\gamma_\rho < \frac{1}{2}$ is given by

$$A_{R,s}(q,\omega) = \begin{cases} C(\omega - u_\rho q)^{\gamma_\rho - \frac{1}{2}} \sin \pi\gamma_\rho & (\omega > u_\rho q), \\ C(u_\rho q - \omega)^{\gamma_\rho - \frac{1}{2}} & (\omega < u_\rho q), \end{cases} \tag{4.25}$$

and the asymptotic behavior for $\frac{1}{2} < \gamma_\rho < 1$ is given by

$$A_{R,s}(q,\omega) = \begin{cases} A_{R,s}(q,u_\rho q) - C'(\omega - u_\rho q)^{\gamma_\rho - \frac{1}{2}} \sin \pi\gamma_\rho & (\omega \geqslant u_\rho q), \\ A_{R,s}(q,u_\rho q) - C'(u_\rho q - \omega)^{\gamma_\rho - \frac{1}{2}} & (\omega \leqslant u_\rho q), \end{cases} \tag{4.26}$$

where C and C' are positive numerical constants depending on q. Because of our simplified treatment of the cutoff, the sum rule $\int d\omega\, A(q,\omega) = 1$ cannot be satisfied. In a more rigorous treatment, the short-range cutoff α used in the construction of the creation and annihilation operators[74] and the momentum cutoff for the interactions must be treated independently.[8] However, in our paper, we are only concerned with the asymptotic behavior of the spectral functions for momenta that deviate from the Fermi momenta by an amount which is much less that the momentum cutoff. In such a case, the corrections resulting from having two-distinct cutoffs can be safely ignored.

B. General two-band model

Next we consider the case of a general two-band model, and evaluate the integral (4.9). By using twice the Feynman identity (4.13) and Eq. (A4), we can reexpress Eq. (4.9) as

$$\begin{aligned} I_{R,a}(q,\omega) = {} & \frac{\alpha^{\bar{\nu}_a - 1}}{\Gamma(\nu_{a,+})\Gamma(\nu_{a,-})\Gamma(\nu'_{a,+})\Gamma(\nu'_{a,-})} \int_0^1 dw_1 \int_0^1 dw_2 \\ & \times w_1^{\nu_{a,+}-1}(1-w_1)^{\nu_{a,-}-1} w_2^{\nu'_{a,+}-1}(1-w_2)^{\nu'_{a,-}-1} \\ & \times [\omega - u(w_1)q]^{\nu'_{a,+}+\nu'_{a,-}-1}[\omega + u(w_2)q]^{\nu_{a,+}+\nu_{a,-}-1} \\ & \times \frac{\Theta[\omega - u(w_1)q]\Theta[\omega + u(w_2)q]}{[u(w_1) + u(w_2)]^{\bar{\nu}_a - 1}}, \end{aligned} \tag{4.27}$$

where $u(w) \equiv wu_+ + (1-w)u_-$. From Eq. (4.27), we obtain $A_{R,a}(q > 0, |\omega| < u_- q) = 0$. Contrary to the SU(2) symmetric case of Sec. IV A, the spectral function does not vanish anymore when $-u_+ q < \omega < -u_- q$.

1. Power-law singularities

The power-law singularities[49,50] can be recovered from Eq. (4.27) in a simple manner. In the analysis of the power-law

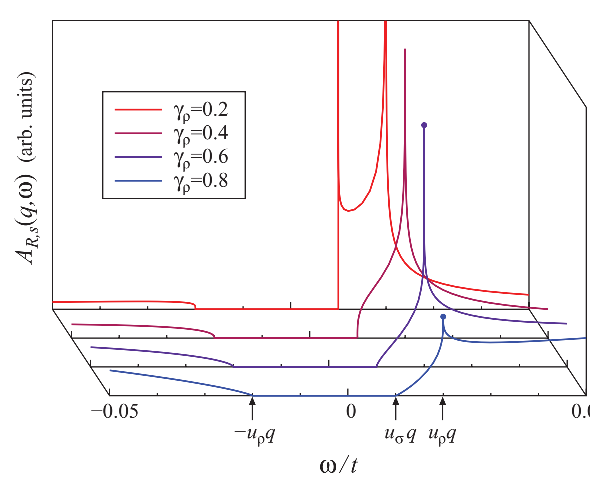

FIG. 3. (Color online) Spectral functions $A_{R,s}(q = 0.01,\omega)$ with SU(2) symmetry for several choices of γ_ρ (=0.2, 0.4, 0.6, and 0.8 from top to bottom) with fixed $u_\rho = 2$, $u_\sigma = 1$, and $q = 0.01$. The dots represent the value at $\omega = u_\rho q$ given by Eq. (4.24).

singularities, we restrict ourselves to the case $q > 0$. Indeed, if we consider the case of $\omega \to u_+ q + 0$, the dominant contribution to the integral comes from the integration over w_1 in the vicinity of $w_1 = 1$. The integral to consider is then

$$I_{R,a}(q,\omega) \propto \int_0^1 dw_1 (1 - w_1)^{\nu_{a,-}-1} \times [(\omega - u_+ q) + \Delta u q (1 - w_1)]^{\nu'_{a,-}+\nu'_{a,+}-1} \approx |\omega - u_+ q|^{\nu_{a,-}+\nu'_{a,-}+\nu'_{a,+}-1} |\Delta u q|^{-\nu_{a,-}}, \tag{4.28}$$

provided that $\nu_{a,-} + \nu'_{a,-} + \nu'_{a,+} < 1$, where $\Delta u \equiv (u_+ - u_-)$. Similarly, when $u_- q < \omega < u_+ q$, the w_1 integration also determines the power-law singularities. This time, the integration over w_1 is restricted to $0 < w_1 < (\omega - u_- q)/(\Delta u q)$. Changing variables to $\bar{w}_1 = w_1(\omega - u_- q)/(\Delta u q)$, we have to consider the integral:

$$\frac{(\omega - u_- q)^{\nu_{a,+}+\nu'_{a,-}+\nu'_{a,+}-1}}{(\Delta u q)^{\nu_{a,+}-1}} \int_0^1 d\bar{w}_1 \bar{w}_1^{\nu_{a,+}-1} \times (1 - \bar{w}_1)^{\nu'_{a,-}+\nu'_{a,+}-1} \left(1 - \frac{\omega - u_- q}{\Delta u q} \bar{w}_1\right)^{\nu_{a,-}-1}. \tag{4.29}$$

When $\omega \to u_- q + 0$, the integral goes to a constant, and we have the power law: $I_{R,a}(q,\omega) \sim (\omega - u_- q)^{\nu_{a,+}+\nu'_{a,+}+\nu'_{a,-}-1}$. When $\omega \to u_+ q - 0$, the integral has a power-law singularity, and the behavior $I_{R,a}(q,\omega) \sim (-\omega + u_+ q)^{\nu_{a,-}+\nu'_{a,+}+\nu'_{a,-}-1}$ is obtained. Such behavior was previously obtained in Refs. 49 and 50. By a similar method, one can also obtain the power-law singularities at $\omega = -u_\pm q$ of $I_{R,a}(-q,-\omega)$. This time, the origin of the singularities is the integration over w_2. By summarizing, the asymptotic behavior of the spectral function is given by

$$A_{R,a}(q,\omega) \propto \begin{cases} |\omega - u_+ q|^{\beta_{a,+}} & (\text{for } \omega \to +u_+ q \pm 0), \\ (\omega - u_- q)^{\beta_{a,-}} & (\text{for } \omega \to +u_- q + 0), \\ (\omega + u_- q)^{\beta'_{a,-}} & (\text{for } \omega \to -u_- q - 0), \\ C + |\omega + u_+ q|^{\beta'_{a,+}} & (\text{for } \omega \to -u_+ q \pm 0), \end{cases} \tag{4.30}$$

where

$$\beta_{a,+} \equiv \nu_{a,-} + \nu'_{a,+} + \nu'_{a,-} - 1, \tag{4.31a}$$
$$\beta_{a,-} \equiv \nu_{a,+} + \nu'_{a,+} + \nu'_{a,-} - 1, \tag{4.31b}$$
$$\beta'_{a,-} \equiv \nu_{a,+} + \nu_{a,-} + \nu'_{a,+} - 1, \tag{4.31c}$$
$$\beta'_{a,+} \equiv \nu_{a,+} + \nu_{a,-} + \nu'_{a,-} - 1. \tag{4.31d}$$

As $\nu_{a,+} + \nu_{a,-} = 1 + \nu'_{a,+} + \nu'_{a,-}$, there is no divergence but only a cusp in the vicinity of $\omega = -u_\pm q$. From Eq. (4.7), the exponents that determine the Green's function for the right-moving particle in Eqs. (4.9) are given by

$$\nu_{1,\pm} = \frac{1}{8}\left(\frac{K_1 u_1}{u_\pm} + \frac{u_\pm}{K_1 u_1} + 2\right)\left(1 \pm \frac{u_1^2 - u_2^2}{u_+^2 - u_-^2}\right),$$
$$\nu'_{1,\pm} = \frac{1}{8}\left(\frac{K_1 u_1}{u_\pm} + \frac{u_\pm}{K_1 u_1} - 2\right)\left(1 \pm \frac{u_1^2 - u_2^2}{u_+^2 - u_-^2}\right),$$

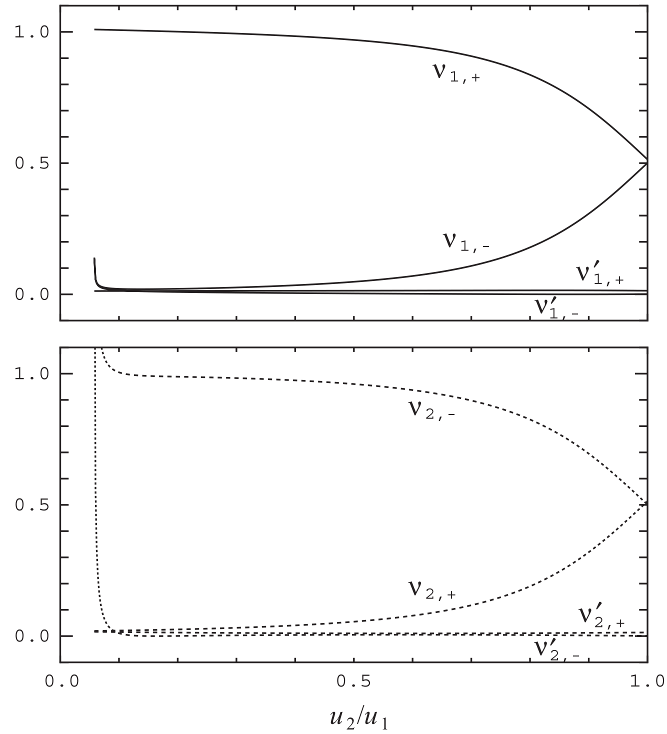

FIG. 4. u_2/u_1 dependence of the exponents $\nu_{1,\pm}$, $\nu'_{1,\pm}$ (top) and $\nu_{2,\pm}$, $\nu'_{2,\pm}$ (bottom) for $K_1 = K_2 = 0.8$ and $g/(\pi u_1) = 0.3$. The two-component TL liquid is unstable for $u_2 < u_{2c} \approx 0.0576 u_1$.

$$\nu_{2,\pm} = \frac{1}{8}\left(\frac{K_2 u_2}{u_\pm} + \frac{u_\pm}{K_2 u_2} + 2\right)\left(1 \mp \frac{u_1^2 - u_2^2}{u_+^2 - u_-^2}\right),$$
$$\nu'_{2,\pm} = \frac{1}{8}\left(\frac{K_2 u_2}{u_\pm} + \frac{u_\pm}{K_2 u_2} - 2\right)\left(1 \mp \frac{u_1^2 - u_2^2}{u_+^2 - u_-^2}\right). \tag{4.32}$$

Figure 4 shows the exponents $\nu_{a,\beta}$ [Eq. (4.32)] as a function of difference in velocities. In order to distinguish the effects of the intraband coupling g_a and the interband coupling g, we plot the u_2/u_1 dependence of the exponents with fixed K_a (i.e., fixed g_a/v_a). In this case, the two-component TL liquid is always unstable for small u_2, in contrast to the situation in Fig. 2. For $u_1 = u_2$, the behavior is similar to that of the TL liquid with only the intraband forward scattering where $(\nu_{a,+},\nu_{a,-},\nu'_{a,+},\nu'_{a,-}) \approx (0.514, 0.501, 0.014, 0.001)$, suggesting the weak effect of the intraband interactions. With decreasing u_2, the exponent $\nu_{1,-}$ ($\nu_{2,+}$) decreases, suggesting that the integral at $x \approx u_- t$ ($x \approx u_+ t$) for $I_{R,1}$ ($I_{R,2}$) in Eq. (4.9) becomes less singular. Although the effect of intraband interaction on $\nu'_{1,\pm}$ and $\nu'_{2,\pm}$ is small for $u_2/u_1 \simeq 1$, the exponents $\nu'_{1,-}$ and $\nu'_{2,-}$ are enhanced for small u_2 just above u_{2c}. In Fig. 5, the corresponding $\beta_{1,\pm}$, $\beta_{2,\pm}$, $\beta'_{1,\pm}$, and $\beta'_{2,\pm}$ are shown. The case of $K = 1$ (not shown) is similar to Fig. 5. Note that the exponent $\nu'_{1,+}$ becomes extremely small but nonzero for $K_1 = K_2 = 1$ and small g/π. Its asymptotic behavior is given by $\nu'_{1,+} \simeq [g/(\pi u_1)]^4 (u_2/u_1)^2/16$ for $u_2 \ll u_1$.

As will be shown in the next section, the spectral function has two divergences at $\omega = u_+ q$ and $\omega = u_- q$ when $\beta_{2,+} < 0$ and $\beta_{1,-} < 0$, respectively. However, each divergence is replaced by a cusp when $\beta_{2,+} > 0$ and $\beta_{1,-} > 0$, respectively. Figure 6 shows such a critical value as a function of $g/(\pi u_1)$ with fixed $\beta_{2,+} = 0$ (solid lines) and $\beta_{1,-} = 0$ (dotted lines) for two cases where the intraband interaction is absent ($K_1 = K_2 = 1$) and is present ($K_1 = K_2 = 0.8$). For $K_a = 1$, the critical value of u_2 increases as a function of g, while that takes a minimum for $K = 0.8$. The minimum for $K \neq 1$ suggests a competition between the intraband interaction and the interband interaction. With increasing K to 1, the value of $g/(\pi u_1)$ at which u_2 takes a minimum decreases, and the line in the limit of $K \to 1$ coincides with that of $K = 1$ except for $g/\pi = 0$, where $u_2/u_1 = 1$ at $g/\pi = 0$ is always obtained for $K \neq 0$. Thus, it is found that double peaks of the spectral functions of fermions in either band are replaced by a single peak in the region enclosed by the solid line and the dotted line in Fig. 6.

2. *Representation of spectral function as integrals of hypergeometric functions*

It is possible to rewrite the double integral (4.27) as a single integral containing the Gauss hypergeometric function[75] ${}_2F_1(\alpha,\beta;\gamma;z)$ (see Appendix A). We again restrict ourselves to the case of $q > 0$. The spectral function for $q < 0$ can be easily obtained by noting $A_{\nu,a}(q,\omega) = A_{\nu,a}(-q,-\omega)$ [see Eq. (4.3)]. For $|\omega| > u_+q$, we obtain

$$A_{R,a}(q,\omega)|_{\omega>u_+q} = \frac{(q\alpha)^{\bar{\nu}_a-1}}{\Gamma(\nu_{a,+}+\nu_{a,-})\Gamma(\nu'_{a,+})\Gamma(\nu'_{a,-})} \frac{(\omega-u_+q)^{\nu_{a,-}+\nu'_{a,+}+\nu'_{a,-}-1}(\omega+u_+q)^{\nu_{a,+}+\nu_{a,-}-1}}{(\omega-u_-q)^{\nu_{a,-}}(2u_+q)^{\nu_{a,+}+\nu_{a,-}+\nu'_{a,+}-1}(2\bar{u}q)^{\nu'_{a,-}}} \times \int_0^1 dt\ (1-t)^{\nu'_{a,+}-1}(t)^{\nu'_{a,-}-1}\left[1+\frac{\Delta u(\omega-u_+q)}{2\bar{u}(\omega+u_+q)}t\right]^{\nu_{a,+}+\nu_{a,-}-1} {}_2F_1(\bar{\nu}_a-1,\nu_{a,-};\nu_{a,+}+\nu_{a,-};z_1), \tag{4.33a}$$

$$A_{R,a}(q,\omega)|_{\omega<-u_+q} = \frac{(q\alpha)^{\bar{\nu}_a-1}}{\Gamma(\nu'_{a,+}+\nu'_{a,-})\Gamma(\nu_{a,+})\Gamma(\nu_{a,-})} \frac{(|\omega|-u_+q)^{\nu_{a,+}+\nu_{a,-}+\nu'_{a,-}-1}(|\omega|+u_+q)^{\nu'_{a,+}+\nu'_{a,-}-1}}{(|\omega|-u_-q)^{\nu'_{a,-}}(2u_+q)^{\nu_{a,+}+\nu'_{a,+}+\nu'_{a,-}-1}(2\bar{u}q)^{\nu_{a,-}}} \times \int_0^1 dt\ (1-t)^{\nu_{a,+}-1}(t)^{\nu_{a,-}-1}\left[1+\frac{\Delta u(|\omega|-u_+q)}{2\bar{u}(|\omega|+u_+q)}t\right]^{\nu'_{a,+}+\nu'_{a,-}-1} {}_2F_1(\bar{\nu}_a-1,\nu'_{a,-};\nu'_{a,+}+\nu'_{a,-};z_1). \tag{4.33b}$$

Here $\bar{u} \equiv (u_+ + u_-)/2$ and $\Delta u \equiv (u_+ - u_-)$. The parameter z_1 is given by

$$z_1 = \frac{\Delta u(|\omega|+u_+q)}{2u_+(|\omega|-u_-q)}\left[1+\frac{\Delta u(|\omega|-u_+q)}{2\bar{u}(|\omega|+u_+q)}t\right]. \tag{4.34}$$

For $u_-q < |\omega| < u_+q$, we have

$$A_{R,a}(q,\omega)|_{u_-q<\omega<u_+q} = \frac{(q\alpha)^{\bar{\nu}_a-1}}{\Gamma(\nu_{a,+}+\nu'_{a,+}+\nu'_{a,-})\Gamma(\nu_{a,-})B(\nu'_{a,+},\nu'_{a,-})} \frac{(\omega-u_-q)^{\nu_{a,+}+\nu'_{a,+}+\nu'_{a,-}-1}(-\omega+u_+q)^{\nu_{a,-}+\nu'_{a,-}+\nu'_{a,+}-1}}{(\omega+u_+q)^{\nu'_{a,+}}(\omega+u_-q)^{\nu'_{a,-}}(\Delta uq)^{\bar{\nu}_a-1}} \times \int_0^1 dt\ (1-t)^{\nu'_{a,+}-1}(t)^{\nu'_{a,-}-1} {}_2F_1(\bar{\nu}_a-1,\nu'_{a,+}+\nu'_{a,-};\nu_{a,+}+\nu'_{a,+}+\nu'_{a,-};z_2), \tag{4.35a}$$

$$A_{R,a}(q,\omega)|_{-u_+q<\omega<-u_-q} = \frac{(q\alpha)^{\bar{\nu}_a-1}}{\Gamma(\nu_{a,+}+\nu_{a,-}+\nu'_{a,+})\Gamma(\nu'_{a,-})B(\nu_{a,+},\nu_{a,-})} \frac{(|\omega|-u_-q)^{\nu_{a,+}+\nu_{a,-}+\nu'_{a,+}-1}(-|\omega|+u_+q)^{\nu_{a,+}+\nu_{a,-}+\nu'_{a,-}-1}}{(|\omega|+u_+q)^{\nu_{a,+}}(|\omega|+u_-q)^{\nu_{a,-}}(\Delta uq)^{\bar{\nu}_a-1}} \times \int_0^1 dt\ (1-t)^{\nu_{a,+}-1}(t)^{\nu_{a,-}-1} {}_2F_1(\bar{\nu}_a-1,\nu_{a,+}+\nu_{a,-};\nu_{a,+}+\nu_{a,-}+\nu'_{a,+};z_2), \tag{4.35b}$$

where $B(p,q)$ is the beta function $B(p,q) = \Gamma(p)\Gamma(q)/\Gamma(p+q)$. The parameter z_2 is given by

$$z_2 = \frac{2u_+(|\omega|-u_-q)}{\Delta u(|\omega|+u_+q)}\left[1+\frac{\Delta u(-|\omega|+u_+q)}{2u_+(|\omega|+u_-q)}t\right]. \tag{4.36}$$

We find $A_{R,a}(q,\omega)|_{-u_-q<\omega<u_-q} = 0$. We note that, if $\nu'_{a,-} = 0$, we have $A_{R,a} = 0$ for $-u_+q < \omega < -u_-q < 0$. In Eq. (4.33), the power-law singularities are already factored out and the integrals are regular. This fact allows for the numerical evaluation of the formulas (4.33) and (4.35). The integrals in Eq. (4.33) can also be reduced to the Appell hypergeometric functions.[76,77] By using Eq. (A11), the spectral functions for the range $u_-q < |\omega| < u_+q$ are expressed as

$$A_{R,a}(q,\omega)|_{u_-q<\omega<u_+q} = \frac{(\alpha/\Delta u)^{\bar{\nu}_a-1}}{\Gamma(\nu_{a,+}+\nu'_{a,+}+\nu'_{a,-})\Gamma(\nu_{a,-})} \frac{(|\omega|-u_-q)^{\nu_{a,+}+\nu'_{a,-}+\nu'_{a,+}-1}(-|\omega|+u_+q)^{\nu_{a,-}+\nu'_{a,-}+\nu'_{a,+}-1}}{(|\omega|+u_+q)^{\nu'_{a,+}}(|\omega|+u_-q)^{\nu'_{a,-}}} \times F_1\left(\bar{\nu}_a-1;\nu'_{a,+},\nu'_{a,-};\nu_{a,+}+\nu'_{a,+}+\nu'_{a,-};\frac{2u_+(|\omega|-u_-q)}{\Delta u(|\omega|+u_+q)},\frac{2\bar{u}(|\omega|-u_-q)}{\Delta u(|\omega|+u_-q)}\right), \tag{4.37}$$

$$A_{R,a}(q,\omega)|_{-u_+q<\omega<-u_-q} = \frac{(\alpha/\Delta u)^{\bar{\nu}_a-1}}{\Gamma(\nu_{a,+}+\nu_{a,-}+\nu'_{a,+})\Gamma(\nu'_{a,-})} \frac{(|\omega|-u_-q)^{\nu_{a,+}+\nu_{a,-}+\nu'_{a,+}-1}(-|\omega|+u_+q)^{\nu_{a,+}+\nu_{a,-}+\nu'_{a,-}-1}}{(|\omega|+u_+q)^{\nu_{a,+}}(|\omega|+u_-q)^{\nu_{a,-}}} \times F_1\left(\bar{\nu}_a-1;\nu_{a,+},\nu_{a,-};\nu_{a,+}+\nu_{a,-}+\nu'_{a,+};\frac{2u_+(|\omega|-u_-q)}{\Delta u(|\omega|+u_+q)},\frac{2\bar{u}(|\omega|-u_-q)}{\Delta u(|\omega|+u_-q)}\right), \tag{4.38}$$

where $F_1(\alpha;\beta,\beta';\gamma;x,y)$ is the first Appell hypergeometric function of two variables. Similarly, by using Eq. (A12), Eq. (4.35) can also be reduced to

$$A_{R,a}(q,\omega)|_{\omega>u_+q} = \frac{(\alpha/2u_+)^{\bar{\nu}_a-1}}{\Gamma(\nu_{a,+}+\nu_{a,-})\Gamma(\nu'_{a,+}+\nu'_{a,-})} \frac{(|\omega|-u_+q)^{\nu_{a,-}+\nu'_{a,+}+\nu'_{a,-}-1}(|\omega|+u_+q)^{\nu_{a,+}+\nu_{a,-}+\nu'_{a,-}-1}}{(|\omega|-u_-q)^{\nu_{a,-}}(|\omega|+u_-q)^{\nu'_{a,-}}} \times F_2\left(\bar{\nu}_a-1;\,\nu_{a,-},\,\nu'_{a,-},\,\nu_{a,+}+\nu_{a,-},\,\nu'_{a,+}+\nu'_{a,-};\,\frac{\Delta u(|\omega|+u_+q)}{2u_+(|\omega|-u_-q)},\frac{\Delta u(|\omega|-u_+q)}{2u_+(|\omega|+u_-q)}\right), \tag{4.39}$$

$$A_{R,a}(q,\omega)|_{\omega<-u_+q} = \frac{(\alpha/2u_+)^{\bar{\nu}_a-1}}{\Gamma(\nu'_{a,+}+\nu'_{a,-})\Gamma(\nu_{a,+}+\nu_{a,-})} \frac{(|\omega|-u_+q)^{\nu_{a,+}+\nu_{a,-}+\nu'_{a,-}-1}(|\omega|+u_+q)^{\nu_{a,-}+\nu'_{a,+}+\nu'_{a,-}-1}}{(|\omega|-u_-q)^{\nu'_{a,-}}(|\omega|+u_-q)^{\nu_{a,-}}} \times F_2\left(\bar{\nu}_a-1;\,\nu'_{a,-},\,\nu_{a,-};\,\nu'_{a,+}+\nu'_{a,-},\,\nu_{a,+}+\nu_{a,-};\,\frac{\Delta u(|\omega|+u_+q)}{2u_+(|\omega|-u_-q)},\frac{\Delta u(|\omega|-u_+q)}{2u_+(|\omega|+u_-q)}\right), \tag{4.40}$$

where $F_2(\alpha;\beta,\beta';\gamma,\gamma';x,y)$ is the second Appell hypergeometric function.[76,77] These results are reminiscent of the one from Ref. 78, where the Fourier transform of the $2k_F$ component of the density-density correlation function of a TL liquid with different spin and charge velocities was shown to be expressible in terms of the Appell hypergeometric function of two variables. We note also that by setting $u_+ = u_\rho$, $u_- = u_\sigma$, $\nu_{a,+} = (\gamma_\rho + 1/2)$, $\nu_{a,-} = 1/2$, $\nu'_{a,+} = \gamma_\rho$, and $\nu'_{a,-} = 0$ in Eqs. (4.37), (4.39), and (4.40), we can reproduce Eqs. (4.21), (4.18), and (4.23), respectively, showing that the Appell hypergeometric function representation also covers the SU(2) invariant case. The special case of SU(2) symmetry can also be recovered from the integral representations (4.33) and (4.35). However, to do this, we first need to consider the limit $\nu_2 \to 0$ in Eq. (4.13). Rewriting Eq. (4.13) as

$$\frac{1}{A_1^{\nu_1}A_2^{\nu_2}} = \frac{\Gamma(\nu_1+\nu_2)}{\Gamma(\nu_1)\Gamma(\nu_2+1)} \times \int_0^1 dw\,\frac{\nu_2 w^{\nu_2-1}(1-w)^{\nu_1-1}}{[A_1(1-w)+A_2w]^{\nu_1+\nu_2}}, \tag{4.41}$$

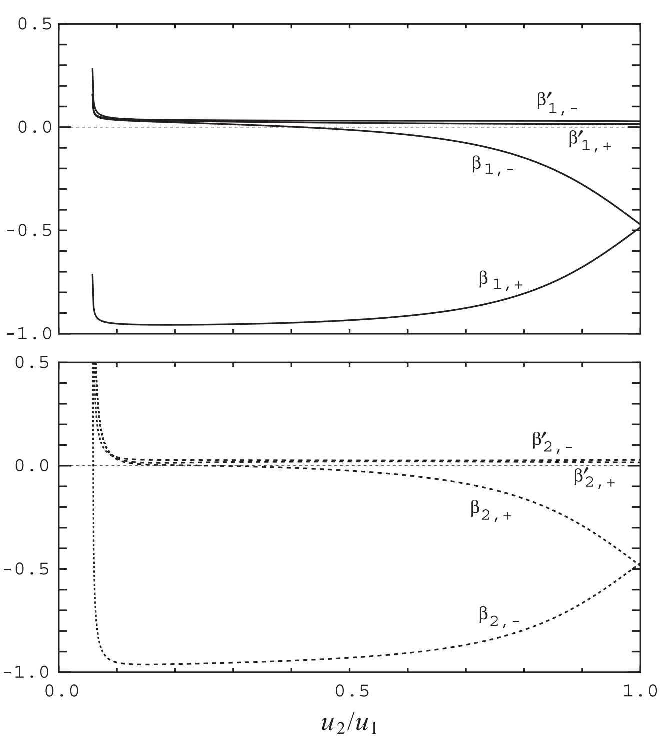

FIG. 5. u_2/u_1 dependence of the exponents $\beta_{1,\pm}$, $\beta'_{1,\pm}$ (top) and $\beta_{2,\pm}$, $\beta'_{2,\pm}$ (bottom) for $K_1 = K_2 = 0.8$ and $g/(\pi u_1) = 0.3$.

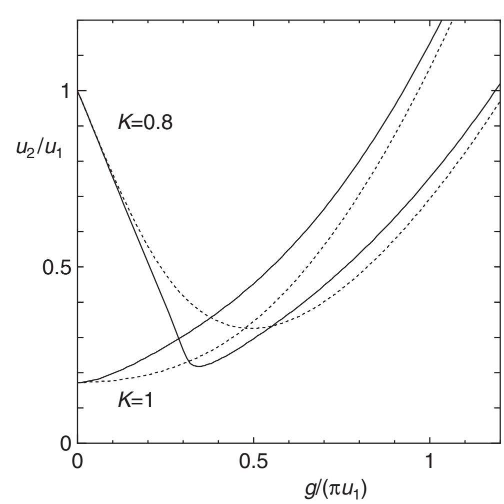

FIG. 6. Values for u_2/u_1 satisfying $\beta_{2,+} = 0$ (solid line) and $\beta_{1,-} = 0$ (dotted line), with fixed $K(= K_1 = K_2) = 1$ and 0.8.

by making $w \to (1-w)$, using $\Gamma(\nu_2+1) = \nu_2\Gamma(\nu_2)$, and changing the integration variable to $v = w^{\nu_2}$, we find that

$$\frac{1}{A_1^{\nu_1} A_2^{\nu_2}} = \frac{\Gamma(\nu_1+\nu_2)}{\Gamma(\nu_1)\Gamma(\nu_2+1)} \times \int_0^1 dv \frac{(1-v^{1/\nu_2})^{\nu_1-1}}{[A_1(1-v^{1/\nu_2}) + A_2 v^{1/\nu_2}]^{\nu_1+\nu_2}}. \quad (4.42)$$

With this form, when $\nu_2 \to 0$, $v^{1/\nu_2} \to 0 \forall v < 1$, and the integral reduces to $A_1^{-\nu_1}$ so that the Feynman identity remains applicable when $\nu_2 \to 0$. By applying the same transformations to Eq. (4.33a), we see that, in the limit of $\nu'_{a-} \to 0$, the SU(2) case is recovered. The same result also applies to Eq. (4.35a). In Eq. (4.33b), when $\nu'_{a+} \to 0$, the hypergeometric function in the integrand reduces to 1. The integral in Eq. (4.33b) thus becomes a hypergeometric function ${}_2F_1$ and the SU(2) invariant case is again recovered. Finally, in Eq. (4.35b), a factor $\Gamma(\nu'_{a,-})$ is present in the denominator of the fraction, but the integral remains finite in the limit $\nu'_{a,-} \to 0$. As a result, in the limit $\nu'_{a,+} \to 0$, the contribution of Eq. (4.35b) to the spectral function vanishes, recovering fully the SU(2) invariant result.

3. *Application to the Hubbard model*

For the application of the present calculation to an explicit model, here we consider the spin-$\frac{1}{2}$ Hubbard model under the magnetic field:

$$H = -t\sum_{j,\sigma}(c^\dagger_{j,\sigma}c_{j+1,\sigma} + \text{H.c.}) - \mu\sum_{j,\sigma} n_{j,\sigma} - h\sum_j (n_{j,\uparrow} - n_{j,\downarrow}) + U\sum_j n_{j,\uparrow}n_{j,\downarrow}, \quad (4.43)$$

where $\sigma = \uparrow,\downarrow$ refers to the spin degrees of freedom. We restrict ourselves to the case of repulsive interaction ($U > 0$). Here we assume that $h > 0$ and the energy dispersion is given by $\varepsilon_{a=1(2)}(k) = -2t\cos k - (+)h - \mu$, where $a = 1$ ($a = 2$) corresponds to the majority (minority) spin. We denote the filling factor by ρ ($0 \leqslant \rho \leqslant 2$). For $h < t(1-\cos\pi\rho)$, two bands are overlapped at Fermi energy. The Fermi momenta and the bare velocities are given by

$$k_{F,1(2)} = \frac{\pi\rho}{2} + (-)\sin^{-1}\left(\frac{h}{2t\sin\frac{\pi\rho}{2}}\right), \quad (4.44)$$

$$u_{1(2)} = 2ta\sin\frac{\pi\rho}{2}\sqrt{1 - \frac{h^2}{4t^2\sin^2\frac{\pi\rho}{2}}} + (-)2ta\cos\frac{\pi\rho}{2}\frac{h}{2t\sin\frac{\pi\rho}{2}}. \quad (4.45)$$

The effective velocities $u_\pm$ are given by Eq. (2.21) with $g = U$ and $K_1 = K_2 = 1$. By considering incommensurate band filling, the umklapp scattering is irrelevant. For $h = 0$, the Hubbard Hamiltonian (4.43) possesses the SU(2) symmetry and the analysis given in Sec. IV A applies. The neglect of the backward scattering can be justified for strong magnetic field, and the effective model can be described by Eq. (2.1) with $g = U$. The magnetic-field dependence of the bare velocities $u_{1,2}$ and the renormalized velocities $u_\pm$ are shown in Fig. 7. For $h = 0$, the velocities u_+ and u_- correspond to the conventional charge v_ρ and spin v_σ excitation velocities, respectively.

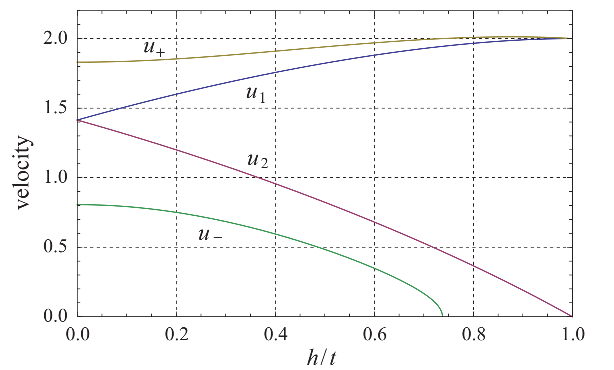

FIG. 7. (Color online) Velocities as a function of the magnetic field for $U/t = 3$ and $\rho = 1/2$.

The spectral functions $A_{R,a}(q,\omega)$ for $h/t = 0.2$ and 0.6 are shown in Fig. 8. In Fig. 9, the contour plot of $A_a(k,\omega)$ is shown in the range $-0.05 < (k - k_{F,a}) < 0.05$ and $-0.05 < \omega/t < 0.05$, with fixed $h/t = 0.2$ (top figures) and 0.6 (bottom figures). The momentum k is related to q by $k = k_{F,a} + q$ [see Eq. (4.3)]. For weak magnetic field, the spectral functions exhibit similar behavior obtained in the SU(2) symmetric case,[49,50] except for the nonzero weight seen at $-u_+q < \omega < -u_-q$. In the SU(2) symmetric case, there is no weight at $-u_+q < \omega < -u_-q$ (see Fig. 3). For strong magnetic field, the difference between u_1 and u_2 becomes large and the spin-up and spin-down electrons are effectively decoupled, where $A_{R,1}$

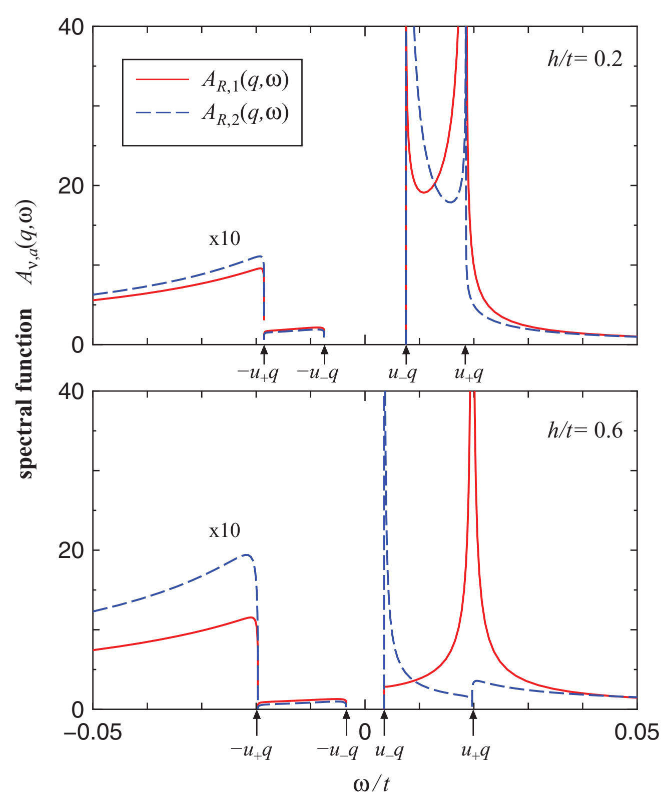

FIG. 8. (Color online) Spectral functions $A_{R,1}(q,\omega)$ and $A_{R,2}(q,\omega)$ for $U/t = 3$ and $q = 0.01/a$, with fixed $h/t = 0.2$ (top) and 0.6 (bottom).

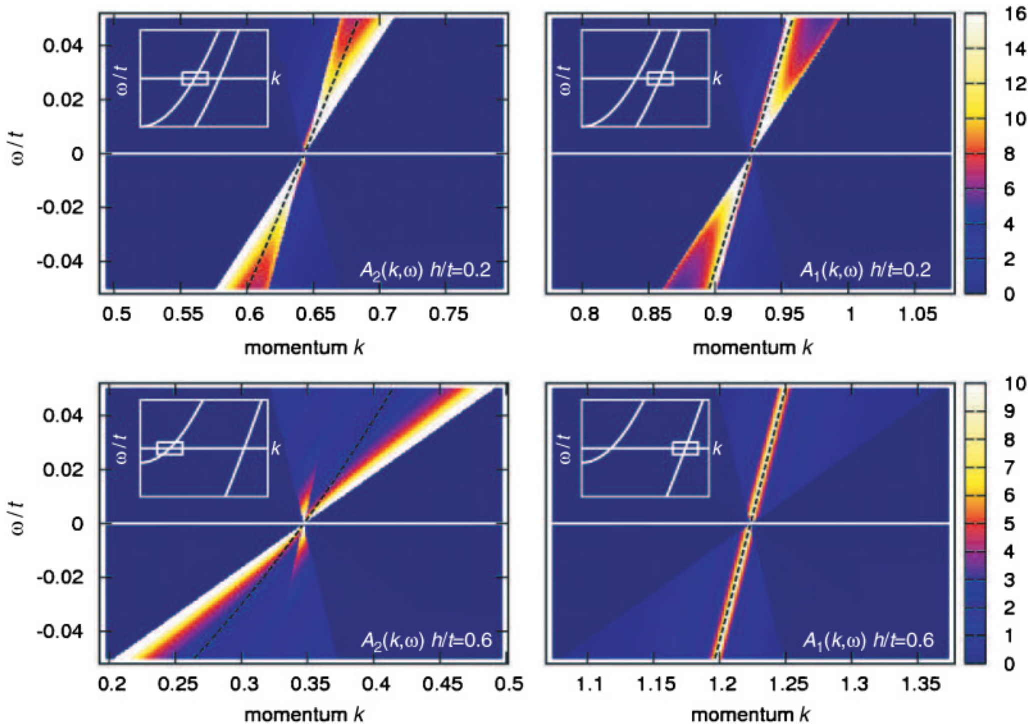

FIG. 9. (Color online) Contour plot of the spectral function $A_a(k,\omega)$ for $a=2$ (left) and $a=1$ (right), with fixed $U/t=3$ and $h/t=0.2$ (top) and $h/t=0.6$ (bottom). The dotted lines denote the bare dispersion $\varepsilon_a(k)\simeq u_a(k-k_{F,a})$ where the Fermi momenta are given by $(k_{F,2},k_{F,1})\simeq(0.64,0.93)$ for $h/t=0.2$ and $(0.35,1.22)$ for $h/t=0.6$. In the insets, the bare energy dispersions are shown and the rectangular represent the region where the spectral functions are plotted in the main figures.

$(A_{R,2})$ has stronger weight at $\omega\approx u_+q$ $(\omega\approx u_-q)$. We note that the weight of $A_{R,2}(q,\omega)$ at $\omega\simeq u_-q$ becomes relatively large compared with that of $A_{R,1}(q,\omega)$ at $\omega\simeq u_+q$, reflecting the large density of states for spin-down particle. Especially, $A_{R,2}(q,\omega)$ exhibits a similar behavior obtained in the spinless case [Fig. 1(a) in Ref. 49]. We also note that, as seen from Fig. 9, the two-branch feature is prominent near Fermi energy $(\omega\simeq 0)$; however, the one-particle feature is recovered in the high-energy region. As seen in Fig. 7, the velocity u_+ takes a close value to u_1, while u_- is strongly renormalized from the bare velocity u_2. For the spectral function $A_2(k,\omega)$, a strong singularity can be seen at $\omega=u_-q$, while relatively large weight can be obtained at $-|u_+q|<\omega<|u_+q|$ for small ω.

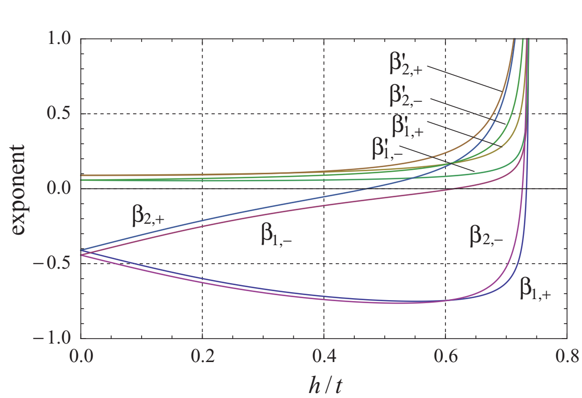

FIG. 10. (Color online) Exponents $\beta_{a,\pm}$ and $\beta'_{a,\pm}$ as a function of the magnetic field for $U/t=3$ and $\rho=1/2$.

By using Eqs. (4.31) and (4.32), the h dependence of the exponents β are obtained (Fig. 10). As mentioned before, the spectral function has two peaks at $\omega=u_+q$ and $\omega=u_-q$ for $\beta_{2,+}<0$ and $\beta_{1,-}<0$, respectively, while each divergence is replaced by a cusp for $\beta_{2,+}>0$ and $\beta_{1,-}>0$, respectively. Figure 11 shows such a critical value of h/t as a function of U/t, for $\beta_{2,+}=0$ (solid line) and $\beta_{1-}=0$ (dotted line). The dash line corresponds to the upper bound of h/t for the stable

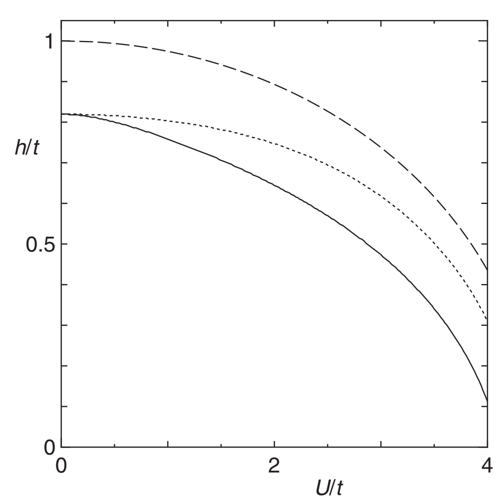

FIG. 11. U dependence of the critical value for h/t satisfying $\beta_{2,+}=0$ (solid line) and $\beta_{1,-}=0$ (dotted line), for $\rho=1/2$. The dash line denotes the upper bound of h/t for the real u_2, i.e., corresponding to u_{2c}.

u_-. With increasing U/t, the critical value of h/t for $\beta_{2,+} = 0$ and $\beta_{1,-} = 0$ decreases.

V. CONCLUSION

In the present paper, we have derived expressions of the fermion spectral functions of a two-component Luttinger liquid at zero temperature in terms of Appell hypergeometric functions. We have shown that, in the SU(2) symmetric case, these expressions reduce to the Gauss hypergeometric functions. Our expressions allow for the recovery of the singularities derived in Refs. 49 and 50, but also describe the amplitude of the singularities as well as the behavior of the spectral function away from the singularities. The results of the present paper could be used to calculate zero temperature fermion spectral functions of various integrable models[79–82] using exact results on the TL-liquid exponents. In the case of three-component models,[83] a more general version of the Feynman identity[73] is applicable, and we expect that the zero-temperature spectral function will also be expressible in terms of generalized hypergeometric functions of three variables. In the case of nonzero temperature, the real-space Green's function is expressed as a product of powers of hyperbolic sines[51] and the Feynman identity[73] we used to derive our expressions does not lead to a tractable expression. However, it is still possible to discuss the qualitative changes to the spectral functions produced by positive temperature. The first effect of being at finite temperature is that the divergences of the spectral functions at $\omega = u_\nu q$ ($\nu = \pm$) are cut off by the thermal length, which is of the order of u_-/T. Therefore, the peaks of the spectral function $A_{R,a}(q,\omega)$ will be replaced by maxima of height $\sim T^{\beta_{a,\nu}}$ as $\omega \to u_\nu q$. For $|\omega - u_\nu q| \gg T$, we expect that the integral giving the spectral function is not strongly affected by the finite temperature as the largest contribution comes from integration over length scales smaller than the thermal length. Therefore, for the lowest (nonzero) temperature scale, we expect that the spectral function will be modified by the replacement of the factor $|\omega - u_\nu q|^{\beta_{a,\nu}}$ by a scaling function $T^{\beta_{a,\nu}}\mathcal{F}_\nu[(\omega - u_\nu q)/T]$ in Eqs. (4.37)–(4.40). The scaling function will be such that $\mathcal{F}_\nu(0)$ is a constant, while $\mathcal{F}_\nu(x) \sim x^{\beta_{a,\nu}}$ when $x \to \infty$. A similar, but weaker, effect should be seen on the cusps at $\omega = -u_\pm q$. Again, the power laws will be replaced by scaling functions that reproduce the infinite slope for $T = 0$. Finally, we expect that the gap $-u_- q < \omega < u_- q$ will start to fill. For higher temperatures, $T \gg |u_+ - u_-|q$, we expect that the difference between the peaks at $\omega = u_\pm q$ becomes blurred, and only a single broad peak will be observed.

ACKNOWLEDGMENTS

E.O. acknowledges discussions with R. Citro and T. Ito. M.T. thanks A. Furusaki for useful comments. M.T. is supported in part by JSPS Institutional Program for Young Researcher Overseas Visits. Y.S. is indebted to the Daiko foundation for the financial aid in the present work. This work was financially supported in part by Grant-in-Aid for Special Coordination Funds for Promoting Science and Technology (SCF), Scientific Research on Innovative Areas 20110002 from the Ministry of Education, Culture, Sports, Science and Technology, Japan.

APPENDIX A: INTEGRALS

1. Fourier transforms

To obtain the spectral functions of the fermions, we need the Fourier transform

$$J(q,\omega) = \int \frac{dx\,dt\,e^{-i(qx-\omega t)}}{[\alpha + i(u_1 t - x)]^{\gamma_1}[\alpha + i(u_2 t + x)]^{\gamma_2}}, \quad \text{(A1)}$$

in the limit of $\alpha \to 0_+$. By the change of variables,

$$t = \frac{X_1 + X_2}{u_1 + u_2}, \quad x = \frac{u_1 X_2 - u_2 X_1}{u_1 + u_2}, \quad \text{(A2)}$$

we find

$$J(q,\omega) = \frac{1}{u_1 + u_2}\int dX_1 \frac{e^{i\frac{(qu_2+\omega)}{u_1+u_2}X_1}}{(\alpha + iX_1)^{\gamma_1}}\int dX_2 \frac{e^{-i\frac{(qu_1-\omega)}{u_1+u_2}X_2}}{(\alpha + iX_2)^{\gamma_2}}. \quad \text{(A3)}$$

The two integrals in the product are obtained from the formula (3.382.7) of Ref. 84, giving the final result,

$$J(q,\omega) = \frac{(2\pi)^2}{\Gamma(\gamma_1)\Gamma(\gamma_2)}\frac{(\omega + u_2 q)^{\gamma_1 - 1}(\omega - u_1 q)^{\gamma_2 - 1}}{(u_1 + u_2)^{\gamma_1+\gamma_2-1}} \times \Theta(\omega - u_1 q)\Theta(\omega + u_2 q), \quad \text{(A4)}$$

where the limit $\alpha \to 0_+$ has been taken.

2. Integrals expressible as hypergeometric functions

The integral representation of the Gauss hypergeometric function is

$${}_2F_1(\alpha,\beta;\gamma;z) = \frac{\Gamma(\gamma)}{\Gamma(\beta)\Gamma(\gamma-\beta)}\int_0^1 dt\,\frac{t^{\beta-1}(1-t)^{\gamma-\beta-1}}{(1-tz)^\alpha}, \quad \text{(A5)}$$

which satisfies [Eq. (15.3.3) in Ref. 75]

$${}_2F_1(\alpha,\beta;\gamma;z) = (1-z)^{\gamma-\alpha-\beta}{}_2F_1(\gamma-\alpha,\gamma-\beta;\gamma;z). \quad \text{(A6)}$$

The typical integral formula for obtaining the spectral functions (4.27) is given by

$$\bar{I} \equiv \int_0^1 dw\,w^{\alpha-1}(1-w)^{\beta-1}\frac{(a+bw)^{\gamma-1}}{(c-bw)^{\alpha+\beta+\gamma-1}}. \quad \text{(A7)}$$

By changing variable $t = 1 - c(1-w)/(c-bw)$, we find

$$\bar{I} = \frac{(a+b)^{\beta+\gamma-1}}{a^\beta(-b+c)^{\alpha+\beta+\gamma-1}}\frac{\Gamma(\alpha)\Gamma(\beta)}{\Gamma(\alpha+\beta)} \times {}_2F_1\left(\alpha+\beta+\gamma-1,\beta;\alpha+\beta;\frac{b(-a-c)}{a(-b+c)}\right), \quad \text{(A8)}$$

where we have used Eqs. (A5) and (A6). For the evaluation of Eq. (4.35), we meet the integral

$$I_1 = \int_0^1 dt\,(1-t)^{\beta-1}t^{\beta'-1}{}_2F_1(a,\beta+\beta';c;\lambda+\mu t). \quad \text{(A9)}$$

By changing the variable t by $t = \lambda\nu/(\lambda+\mu-\mu\nu)$, and by expanding ${}_2F_1(a,b;c;z) = \sum_{n=0}^\infty \frac{(a)_n(b)_n}{(c)_n}\frac{z^n}{n!}$, where

$(a)_n \equiv \Gamma(a+n)/\Gamma(a)$, we find

$$\begin{aligned}
I_1 &= \sum_{n=0}^{\infty}(\lambda+\mu)^{\beta}\lambda^{\beta'}\frac{(a)_n(\beta+\beta')_n}{(c)_n}\frac{[\lambda(\lambda+\mu)]^n}{n!}\int_0^1 d\nu\,\frac{(1-\nu)^{\beta-1}(\nu)^{\beta'-1}}{(\lambda+\mu-\mu\nu)^{\beta+\beta'+n}}\\
&= \frac{\Gamma(\beta)\Gamma(\beta')}{\Gamma(\beta+\beta')}\left(\frac{\lambda}{\lambda+\mu}\right)^{\beta'}\sum_{n=0}^{\infty}\frac{1}{n!}\frac{(a)_n(\beta+\beta')_n}{(c)_n}{}_2F_1\left(\beta+\beta'+n,\beta';\beta+\beta';\frac{\mu}{\lambda+\mu}\right)\lambda^n\\
&= \frac{\Gamma(\beta)\Gamma(\beta')}{\Gamma(\beta+\beta')}\left(\frac{\lambda}{\lambda+\mu}\right)^{\beta'}\sum_{n,m=0}^{\infty}\frac{(\beta+\beta')_{n+m}(a)_n(\beta')_m}{(c)_n(\beta'+\beta)_m}\frac{\lambda^n}{n!}\frac{(\frac{\mu}{\lambda+\mu})^m}{m!}\\
&= \frac{\Gamma(\beta)\Gamma(\beta')}{\Gamma(\beta+\beta')}\left(\frac{\lambda}{\lambda+\mu}\right)^{\beta'}F_2\left(\beta+\beta';a,\beta';c,\beta+\beta';\lambda,\frac{\mu}{\lambda+\mu}\right),
\end{aligned} \tag{A10}$$

where F_2 is the Appell hypergeometric function. By using the relation $F_2(A;B,B';C,A;x,y)=(1-y)^{-B'}F_1[B;A-B',B';C;x,x/(1-y)]$, we obtain

$$I_1 = B(\beta,\beta')F_1(a;\beta,\beta';c;\lambda,\lambda+\mu), \tag{A11}$$

where F_1 is the Appell hypergeometric function. Similarly, the integral in Eq. (4.33) can be performed as

$$\begin{aligned}
I_2 &= \int_0^1 dt\,(1-t)^{\beta-1}t^{\beta'-1}\left(1+\frac{\mu}{\lambda}t\right)^{c-1}{}_2F_1(\beta+\beta'+c-1,b;c;\lambda+\mu t)\\
&= \sum_{n=0}^{\infty}\left(\frac{\lambda}{\lambda+\mu}\right)^{\beta'}\frac{(\beta+\beta'+c-1)_n(b)_n}{(c)_n}\frac{\lambda^n}{n!}\int_0^1 d\nu\,(1-\nu)^{\beta-1}(\nu)^{\beta'-1}\left(1-\frac{\mu\nu}{\lambda+\mu}\right)^{-(\beta+\beta'+c-1+n)}\\
&= \sum_{n=0}^{\infty}\left(\frac{\lambda}{\lambda+\mu}\right)^{\beta'}\frac{(\beta+\beta'+c-1)_n(b)_n}{(c)_n}\frac{\lambda^n}{n!}B(\beta,\beta')\,{}_2F_1\left(\beta+\beta'+c-1+n,\beta';\beta+\beta';\frac{\mu}{\lambda+\mu}\right)\\
&= \left(\frac{\lambda}{\lambda+\mu}\right)^{\beta'}B(\beta,\beta')\sum_{n,m=0}^{\infty}\frac{\lambda^n}{n!}\frac{(\frac{\mu}{\lambda+\mu})^n}{m!}(\beta+\beta'+c-1)_{n+m}\frac{(b)_n(\beta')_m}{(c)_n(\beta+\beta')_m}\\
&= \left(\frac{\lambda}{\lambda+\mu}\right)^{\beta'}B(\beta,\beta')F_2\left(\beta+\beta'+c-1;b,\beta';c,\beta+\beta';\lambda,\frac{\mu}{\lambda+\mu}\right).
\end{aligned} \tag{A12}$$

APPENDIX B: FINITE-SIZE BOSONIZATION AND EXPONENTS

It is well known in conformal field theory that there is a relation between the energy-momentum tensor and the Virasoro generators that gives the conformal weights (or dimensions) of the operators.[85,86] As a result, it is possible to relate the dimension of a given operator to the energy of the state generated by acting on the ground state of the Hamiltonian of a conformally invariant model with that operator.[87] Multicomponent models are not in general conformally invariant, but their critical properties can be obtained by considering a semidirect product of Virasoro algebras.[88] A more elementary approach, that we will follow here, uses finite-size bosonization.[74,89] In that approach, the fields ϕ_a and θ_a in Eq. (2.4) admit the decomposition

$$\phi_a(x) = \phi_0^{(a)} - \frac{\pi n_a}{L}x + \frac{1}{\sqrt{L}}\sum_q \phi_a(q)e^{iqx}, \tag{B1a}$$

$$\theta_a(x) = \theta_0^{(a)} - \frac{\pi J_a}{L}x + \frac{1}{\sqrt{L}}\sum_q \theta_a(q)e^{iqx}. \tag{B1b}$$

In Eqs. (B1), we have the commutation relations $[\phi_0^{(a)},J_b]=-i\delta_{ab}$ and $[\theta_0^{(a)},n_b]=-i\delta_{ab}$. In the Hamiltonian, ϕ_0^a and $\theta_0^{(a)}$

do not appear as a result of the derivations, but there is an extra term:

$$\delta H = \frac{\pi}{2L}\sum_{a,b}(M_{ab}J_aJ_b + N_{ab}n_an_b) = \frac{\pi}{2L}({}^t\boldsymbol{J}M\boldsymbol{J} + {}^t\boldsymbol{n}N\boldsymbol{n}) \tag{B2}$$

$[\boldsymbol{J} = {}^t(J_1,J_2)$ and $\boldsymbol{n} = {}^t(n_1,n_2)]$, which vanishes when $L \to \infty$ and is called the zero-mode contribution. The ground state has $J_a = 0$ and $n_a = 0$. If we consider the momentum operator,

$$P = \sum_a \int dx\, \Pi_a \partial_x \phi_a, \tag{B3}$$

it also contains a zero-mode contribution equal to

$$\delta P = \frac{\pi}{L}\sum_a n_a J_a = \frac{\pi}{L}{}^t\boldsymbol{n}\boldsymbol{J}. \tag{B4}$$

If we use the relations $M = Q(\Delta_2)^{1/2t}Q$ and $N = P(\Delta_2)^{1/2t}P$, we can rewrite

$$\delta H = \frac{\pi}{4L}[({}^t\boldsymbol{J}Q + {}^t\boldsymbol{n}P)(\Delta_2)^{1/2}({}^tQ\boldsymbol{J} + {}^tP\boldsymbol{n}) + ({}^t\boldsymbol{J}Q - {}^t\boldsymbol{n}P)(\Delta_2)^{1/2}({}^tQ\boldsymbol{J} - {}^tP\boldsymbol{n})], \tag{B5}$$

$$\delta P = \frac{\pi}{4L}[({}^t\boldsymbol{J}Q + {}^t\boldsymbol{n}P)({}^tQ\boldsymbol{J} + {}^tP\boldsymbol{n}) - ({}^t\boldsymbol{J}Q - {}^t\boldsymbol{n}P)({}^tQ\boldsymbol{J} - {}^tP\boldsymbol{n})]. \tag{B6}$$

Now, if we act on the ground state with the operator $e^{i\sum_a(\eta_a\theta_a+\xi_a\phi_a)(x)}$, due to the presence of the term $\sum_a(\eta_a\theta_0^{(a)} + \xi_a\phi_0^{(a)})$, the resulting state will belong to the subspace with $n_a = -\eta_a, J_a = -\xi_a$. Its zero-mode contribution to the ground-state energy will be

$$\delta H = \frac{\pi}{4L}\sum_\beta \left[u_\beta({}^t\xi Q + {}^t\eta P)_\beta^2 + u_\beta({}^t\xi Q - {}^t\eta P)_\beta^2\right], \tag{B7}$$

$$\delta P = \frac{\pi}{4L}\left[({}^t\xi Q + {}^t\eta P)_\beta^2 - ({}^t\xi Q - {}^t\eta P)_\beta^2\right]. \tag{B8}$$

For an infinite system, a simple generalization of Eq. (4.8) shows that the correlation function take the form

$$\langle e^{i(\sum_a \eta_a\theta_a+\xi_a\phi_a)(x,t)}e^{-i(\sum_a \eta_a\theta_a+\xi_a\phi_a)(0,0)}\rangle = \prod_\beta \left[\frac{\alpha}{\alpha + i(u_\beta t + x)}\right]^{({}^t\eta P+{}^t\xi Q)_\beta^2/4} \times \left[\frac{\alpha}{\alpha + i(u_\beta t - x)}\right]^{({}^t\eta P-{}^t\xi Q)_\beta^2/4}. \tag{B9}$$

So we see that the dimensions $({}^t\eta P \pm {}^t\xi Q)_\beta^2/4$ in the correlation functions also appear in the zero-mode contributions to the excited-state energy and momentum of the finite-size system. This remark is the basis for the method of Frahm and Korepin.[88] Indeed, Eq. (8.2) of Ref. 88 is recovered with $P = {}^tU^t(Z^{-1})$, where

$$U = \begin{pmatrix} 1 & 1 \\ 0 & 1 \end{pmatrix}, \tag{B10}$$

since Frahm and Korepin have defined $N_c = N_\uparrow + N_\downarrow$ and $N_s = N_\downarrow$, so that

$$\begin{pmatrix} N_c \\ N_s \end{pmatrix} = U \begin{pmatrix} N_\uparrow \\ N_\downarrow \end{pmatrix}. \tag{B11}$$

Similarly, Eq. (3.6) of Ref. 88 is recovered by taking $Q = U^{-1}Z$. Using these definitions, we can recover Eqs. (3.12), (3.11), and (3.13) of Ref. 88. These relations have also been derived in Ref. 72 by comparing the critical exponents derived from the Bethe ansatz with the ones derived from bosonization.

[1] L. D. Landau, Zh. Eksp. Teor. Fiz. **30**, 1058 (1956) [Sov. Phys. JETP **3**, 920 (1957)].
[2] P. Nozières, *Theory of Interacting Fermi Systems* (Benjamin, New York, 1961).
[3] S. Tomonaga, Prog. Theor. Phys. **5**, 544 (1950).
[4] J. M. Luttinger, J. Math. Phys. **4**, 1154 (1963).
[5] H. J. Schulz, in *Mesoscopic Quantum Physics, Les Houches LXI*, edited by E. Akkermans, G. Montambaux, J. L. Pichard, and J. Zinn-Justin (Elsevier, Amsterdam, 1995), p. 533.
[6] J. Voit, Rep. Prog. Phys. **58**, 977 (1995).
[7] C. M. Varma, Z. Nussinov, and W. van Saarloos, Phys. Rep. **361**, 267 (2002).
[8] Y. Suzumura, Prog. Theor. Phys. **63**, 51 (1980).
[9] R. Claessen, M. Sing, U. Schwingenschlögl, P. Blaha, M. Dressel, and C. S. Jacobsen, Phys. Rev. Lett. **88**, 096402 (2002).
[10] T. Ito, A. Chainani, T. Haruna, K. Kanai, T. Yokoya, S. Shin, and R. Kato, Phys. Rev. Lett. **95**, 246402 (2005).
[11] D. Jérome, in *Organic Conductors: Fundamentals and Applications*, edited by J.-P. Farges (Marcel Dekker, New York, 1994), p. 405.
[12] S. Ijima, Nature (London) **354**, 56 (1991).
[13] B. Dardel, D. Malterre, M. Grioni, P. Weibel, Y. Baer, and F. Lévy, Phys. Rev. Lett. **67**, 3144 (1991).
[14] B. Dardel, D. Malterre, M. Grioni, P. Weibel, Y. Baer, J. Voit, and D. Jérome, Europhys. Lett. **24**, 687 (1993).
[15] G. H. Gweon *et al.*, J. Phys. Condens. Matter **8**, 9923 (1996).
[16] T. Mizokawa, K. Nakada, C. Kim, Z.-X. Shen, T. Yoshida, A. Fujimori, S. Horii, Y. Yamada, H. Ikuta, and U. Mizutani, Phys. Rev. B **65**, 193101 (2002).
[17] H. Ishii *et al.*, Nature (London) **426**, 540 (2003).
[18] J. D. Denlinger, G.-H. Gweon, J. W. Allen, C. G. Olson, J. Marcus, C. Schlenker, and L.-S. Hsu, Phys. Rev. Lett. **82**, 2540 (1999).
[19] M. Sing, U. Schwingenschlögl, R. Claessen, P. Blaha, J. M. P. Carmelo, L. M. Martelo, P. D. Sacramento, M. Dressel, and C. S. Jacobsen, Phys. Rev. B **68**, 125111 (2003).
[20] G. H. Gweon, S.-K. Mo, J. W. Allen, J. He, R. Jin, D. Mandrus, and H. Höchst, Phys. Rev. B **70**, 153103 (2004).
[21] M. Grioni, in *Strong Interactions in Low Dimensions*, edited by D. Baeriswyl and L. Degiorgi, Physics and Chemistry of Materials with Low-Dimensional Structures, Vol. 25 (Springer, Heidelberg, Germany, 2004), Chap. 5, p. 137.

[22] V. Vescoli, F. Zwick, W. Henderson, L. DeGiorgi, M. Grioni, G. Gruner, and L. K. Montgomery, Eur. Phys. J. B **13**, 503 (2000).
[23] F. J. Himpsel, K. N. Altmann, R. Bennewitz, J. N. Crain, A. Kirakosian, J.-L. Lin, and J. L. McChesney, J. Phys. Condens. Matter **13**, 11097 (2001).
[24] N. Oncel, J. Phys. Condens. Matter **20**, 393001 (2008).
[25] R. Losio, K. N. Altmann, A. Kirakosian, J.-L. Lin, D. Y. Petrovykh, and F. J. Himpsel, Phys. Rev. Lett. **86**, 4632 (2001).
[26] J. N. Crain, J. L. McChesney, F. Zheng, M. C. Gallagher, P. C. Snijders, M. Bissen, C. Gundelach, S. C. Erwin, and F. J. Himpsel, Phys. Rev. B **69**, 125401 (2004).
[27] T. Okuda *et al.*, Phys. Rev. B **82**, 161410 (2010).
[28] A. Altland, C. H. W. Barnes, F. W. J. Hekking, and A. J. Schofield, Phys. Rev. Lett. **83**, 1203 (1999).
[29] S. A. Grigera, A. J. Schofield, S. Rabello, and Q. Si, Phys. Rev. B **69**, 245109 (2004).
[30] D. Carpentier, C. Peca, and L. Balents, Phys. Rev. B **66**, 153304 (2002).
[31] O. M. Auslaender, H. Steinberg, A. Yacoby, Y. Tserkovnyak, B. I. Halperin, K. W. Baldwin, L. N. Pfeiffer, and K. W. West, Science **308**, 88 (2005).
[32] Y. Jompol, C. J. B. Ford, J. P. Griffiths, I. Farrer, G. A. C. Jones, D. Anderson, D. A. Ritchie, T. W. Silk, and A. J. Schofield, Science **325**, 597 (2009).
[33] A. Recati, P. O. Fedichev, W. Zwerger, and P. Zoller, Phys. Rev. Lett. **90**, 020401 (2003).
[34] A. Recati, P. O. Fedichev, W. Zwerger, and P. Zoller, J. Opt. B: Semiclassical and Quantum Optics **5**, S55 (2003).
[35] C. Kollath and U. Schollwöck, New J. Phys. **8**, 220 (2006).
[36] B. Paredes *et al.*, Nature (London) **429**, 277 (2004).
[37] T. Kinoshita, T. Wenger, and D. S. Weiss, Science **305**, 1125 (2004).
[38] M. Köhl, T. Stöferle, H. Moritz, C. Schori, and T. Esslinger, Appl. Phys. B **79**, 1009 (2004).
[39] A. H. van Amerongen, J. J. P. van Es, P. Wicke, K. V. Kheruntsyan, and N. J. van Druten, Phys. Rev. Lett. **100**, 090402 (2008).
[40] I. Bouchoule, N. J. Van Druten, and C. I. Westbrook, in *Atom Chips* edited by J. Reichel and V. Vuletic (Wiley-VCH Verlag GmbH, Weinheim, 2011), Chap. 11.
[41] K. Günter, T. Stöferle, H. Moritz, M. Köhl, and T. Esslinger, Phys. Rev. Lett. **96**, 180402 (2006).
[42] S. Ospelkaus, C. Ospelkaus, O. Wille, M. Succo, P. Ernst, K. Sengstock, and K. Bongs, Phys. Rev. Lett. **96**, 180403 (2006).
[43] E. Wille *et al.*, Phys. Rev. Lett. **100**, 053201 (2008).
[44] M. Taglieber, A.-C. Voigt, T. Aoki, T. W. Hänsch, and K. Dieckmann, Phys. Rev. Lett. **100**, 010401 (2008).
[45] B. DeMarco and D. S. Jin, Science **285**, 1703 (1999).
[46] Y. Liao, A. S. C. Rittner, T. Paprotta, W. Li, G. B. Partridge, R. G. Hulet, S. K. Baur, and E. J. Mueller, Nature (London) **467**, 567 (2010).
[47] J. T. Stewart, J. P. Gaebler, and D. S. Jin, Nature (London) **454**, 744 (2008).
[48] D. S. Jin, J. T. Stewart, and J. P. Gaebler, in *Pushing the Frontiers of Atomic Physics*, edited by R. Côté, P. L. Gould, M. Rozman, and W. W. Smith (World Scientific, Singapore, 2009), pp. 213–219.
[49] V. Meden and K. Schönhammer, Phys. Rev. B **46**, 15753 (1992).
[50] J. Voit, Phys. Rev. B **47**, 6740 (1993).
[51] N. Nakamura and Y. Suzumura, Prog. Theor. Phys. **98**, 29 (1997).
[52] K. Penc, K. Hallberg, F. Mila, and H. Shiba, Phys. Rev. Lett. **77**, 1390 (1996).
[53] K. Penc, K. Hallberg, F. Mila, and H. Shiba, Phys. Rev. B **55**, 15475 (1997).
[54] M. Ogata and H. Shiba, Phys. Rev. B **41**, 2326 (1990).
[55] K. A. Matveev, A. Furusaki, and L. I. Glazman, Phys. Rev. B **76**, 155440 (2007).
[56] J. Favand, S. Haas, K. Penc, F. Mila, and E. Dagotto, Phys. Rev. B **55**, 4859 (1997).
[57] M. G. Zacher, E. Arrigoni, W. Hanke, and J. R. Schrieffer, Phys. Rev. B **57**, 6370 (1998).
[58] A. Abendschein and F. F. Assaad, Phys. Rev. B **73**, 165119 (2006).
[59] H. Benthien, F. Gebhard, and E. Jeckelmann, Phys. Rev. Lett. **92**, 256401 (2004).
[60] N. Bulut, H. Matsueda, T. Tohyama, and S. Maekawa, Phys. Rev. B **74**, 113106 (2006).
[61] S. Miyashita, A. Kawaguchi, and N. Kawakami, J. Phys. Soc. Jpn. **71**, 1947 (2002).
[62] S. Rabello and Q. Si, Europhys. Lett. **60**, 882 (2002).
[63] A. E. Feiguin and D. A. Huse, Phys. Rev. B **79**, 100507 (2009).
[64] K. A. Muttalib and V. J. Emery, Phys. Rev. Lett. **57**, 1370 (1986).
[65] H. Frahm and V. E. Korepin, Phys. Rev. B **43**, 5653 (1991).
[66] K. Penc and J. Sólyom, Phys. Rev. B **47**, 6273 (1993).
[67] G. Orso, Phys. Rev. Lett. **98**, 070402 (2007).
[68] M. A. Cazalilla and A. F. Ho, Phys. Rev. Lett. **91**, 150403 (2003).
[69] L. Mathey, D.-W. Wang, W. Hofstetter, M. D. Lukin, and E. Demler, Phys. Rev. Lett. **93**, 120404 (2004).
[70] A. O. Gogolin, A. A. Nersesyan, and A. M. Tsvelik, *Bosonization and Strongly Correlated Systems* (Cambridge University Press, Cambridge, UK, 1999).
[71] E. Orignac, M. Tsuchiizu, and Y. Suzumura, Phys. Rev. A **81**, 053626 (2010).
[72] T. Hikihara, A. Furusaki, and K. A. Matveev, Phys. Rev. B **72**, 035301 (2005).
[73] M. Le Bellac, *Quantum and Statistical Field Theory* (Oxford University Press, Oxford, UK, 1992).
[74] F. D. M. Haldane, J. Phys. C **14**, 2585 (1981).
[75] M. Abramowitz and I. Stegun, *Handbook of Mathematical Functions* (Dover, New York, 1972).
[76] A. Erdélyi, W. Magnus, F. Oberhettinger, and F. G. Tricomi, *Higher Transcendental Functions* (McGraw-Hill, New York, 1953), Vol. 1.
[77] R. A. Askey and A. B. Olde Daalhuis, *Digital Library of Mathematical Functions*, edited by Frank W. J. Olver, Daniel W. Lozier, Ronald F. Boisvert, and Charles W. Clark (NIST, Gaithersburg, MD, 2010), Chap. 16.
[78] A. Iucci, G. A. Fiete, and T. Giamarchi, Phys. Rev. B **75**, 205116 (2007).
[79] M. Gaudin, Phys. Lett. A **24**, 55 (1967).
[80] C. N. Yang, Phys. Rev. Lett. **19**, 1312 (1967).
[81] N. Kawakami and S. K. Yang, Phys. Rev. Lett. **65**, 2309 (1990).
[82] A. Imambekov and E. Demler, Ann. Phys. (NY) **321**, 2390 (2006).
[83] A. Luscher and A. Laeuchli, e-print arXiv:0906.0768 (2009).
[84] A. Gradshteyn and R. Ryzhik, *Tables of Integrals, Series and Products* (Academic Press, New York, 1980).
[85] P. Di Francesco, P. Mathieu, and D. Sénéchal, *Conformal Field Theory* (Springer-Verlag, Berlin, 1997).

[86]J. Cardy, *Scaling and Renormalization in Statistical Physics* (Cambridge University Press, Cambridge, UK, 1996).

[87]H. Saleur, in *Topological Aspects of Low Dimensional Systems*, edited by A. Comtet, T. Jolicoeur, S. Ouvry, and F. David, Les Houches Summer School, Vol. 69 (Springer, Berlin, 1998), p. 475.

[88]H. Frahm and V. E. Korepin, Phys. Rev. B **42**, 10553 (1990).

[89]D. Sénéchal, in *Theoretical Methods for Strongly Correlated Electrons*, edited by D. Sénechal *et al.*, CRM Series in Mathematical Physics (Springer, New York, 2003).